

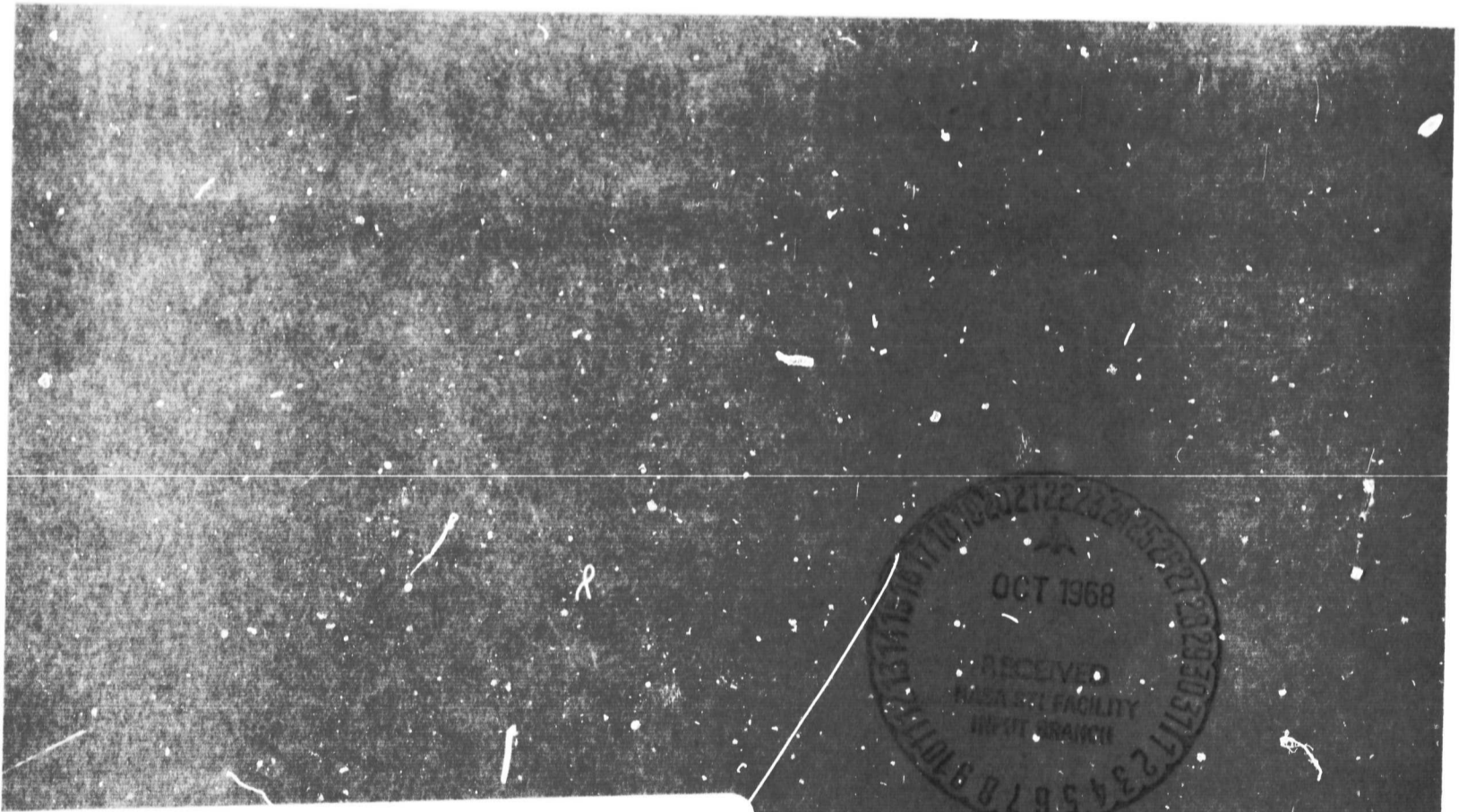
## General Disclaimer

### One or more of the Following Statements may affect this Document

- This document has been reproduced from the best copy furnished by the organizational source. It is being released in the interest of making available as much information as possible.
- This document may contain data, which exceeds the sheet parameters. It was furnished in this condition by the organizational source and is the best copy available.
- This document may contain tone-on-tone or color graphs, charts and/or pictures, which have been reproduced in black and white.
- This document is paginated as submitted by the original source.
- Portions of this document are not fully legible due to the historical nature of some of the material. However, it is the best reproduction available from the original submission.

12044-PR4

# 10.6 MICRON OPTICAL HETERODYNE COMMUNICATION SYSTEM



ACCESSION NUMBER	10791	(THRU)	1
(PAGES)	48	(CODE)	
(NASA CR OR TMX OR AD NUMBER)	CR-98114	(CATEGORY)	07

FACILITY FORM 602

**HONEYWELL SYSTEMS & RESEARCH DIVISION**

Honeywell Report 12044-PR4

31 January 1968

**10.6 MICRON OPTICAL HETERODYNE  
COMMUNICATION SYSTEM**

**Phase 4 Report**

**For Period 1 November through 31 January 1968**

**National Aeronautics and Space Administration  
Marshall Space Flight Center  
Contract No. NAS 8-20645**

Prepared by:

H. W. Mocker

Approved by:



V. S. Levadi  
Aerospace Sciences  
Research Manager

Honeywell Inc.  
Systems and Research Department  
2345 Walnut Street  
Minneapolis, Minnesota 55113

		Page
SECTION 1	INTRODUCTION	1
SECTION 2	THE CO <sub>2</sub> LASER	3
	General Design	3
	Parameter Tradeoff Studies	4
	Dependence of Laser Power and Tube Voltage on the Excitation Current	11
	Laser Beam Spread and Amplitude Stability	19
	Laser Frequency Characteristics	22
SECTION 3	OPTICAL HETERODYNE EXPERIMENTS	34
	Beat Frequency Characteristics	34

## ILLUSTRATIONS

Figure		Page
1	Disassembled View of the Single Mode CO <sub>2</sub> Laser	5
2	Assembled Water - Cooled Laser	6
3	Output Power versus CO <sub>2</sub> Partial Pressure	8
4	Output Power Versus N <sub>2</sub> Partial Pressure	9
5	Output Power versus Helium Partial Pressure	10
6	Output Power versus Excitation Current	12
7	Output Power versus Excitation Current	13
8	Tube Voltage versus Tube Current	14
9	Tube Voltage, Laser Power and Incremental Electrical Power versus Excitation Current	17
10	Single Mode Efficiency versus Excitation Current	18
11	Experimental Setup to Determine Beam Spread and Amplitude Stability	20
12	Intensity Distribution of CO <sub>2</sub> Laser	21
13	Amplitude Stability Measurement	23
14	Amplitude Stability Measurement	24
15	Piezoelectric Tuning Scan for Laser No. 1	27
16	Piezoelectric Tuning Scan for Laser No. 2	28
17	Piezoelectric Tuning Scan for Laser No. 1	29
18	Piezoelectric Tuning Scan for Laser No. 2	30
19	Piezoelectric Tuning Scan of Single Mode	32
20	Single Mode Laser Power versus Piezoelectric Voltage Setting	33

Figure		Page
21	Optical Heterodyne Detection of the Beat Frequency of Two Stable CO <sub>2</sub> Lasers	35
22	Optical Heterodyne Setup Mounted on Granite Slab	36
23	Both Lasers Beating on the P(22) - Transition Horizontal Dispersion 10 k Hz/cm.	38
24	Both Lasers Beating on the P(16) - Transition Horizontal Dispersion (a) 10 k Hz/cm (b) 50 k Hz/cm	39
25	Both Lasers Beating on P(20) - Transition Horizontal Dispersion 50 k Hz/cm.	41
26	Both Lasers Beating on P(18) - Transition Horizontal Dispersion (a) 10 k Hz/cm (b) 100 k Hz/cm	42
27 (a)	Self-beat of Laser No. 1	43
27 (b)	Self-beat (in center) in the Presence of the True Beat Signal	43

#### TABLES

1	Incremental Electrical Power	16
2	Transitions Under Oscillation in Laser 1 and 2	25

## SECTION I INTRODUCTION

This report describes the progress made on the design and construction of a 10.6 micron optical heterodyne communication system during the reporting period from 1 November 1967 to 31 January 1968.

Two water-cooled CO<sub>2</sub> lasers have been built and tested. The lasers oscillated on a power level up to 4.5 watts in a single frequency and zero-order transverse electromagnetic mode. The lasers are diffraction-limited and have a measured beam spread of 2.4 milliradians. Each laser has a piezoelectric element for transition control, with it, 12 to 14 transitions can be brought into oscillation over a tuning range of 450 MHz. The transmitter laser has an additional modulator element, the local oscillator a feedback element in the form of a piezoelectric stack.

A parameter tradeoff study was made to find the best point of operation. Pressure, excitation, gas mixing ratio, and the transition under oscillation have been varied while the output power was measured.

The laser amplitude stability was found to be  $\pm 1$  percent over several hours. Piezoelectric tuning scans yielded the effective frequency width of oscillation for each transition versus applied transducer voltage. For a strong transition, this width is 40-60 MHz and, therefore, sufficient to offset the transmitter and local oscillator by 10 MHz and still allow for sufficient tracking range ( $\pm 10$  MHz) without experiencing transition jumps on either laser.

The heterodyne beat signal from both lasers was obtained on a HgCdTe detector. The short-term fluctuations (1/10 sec) are within 2 parts in  $10^{10}$ . Water-cooling improved the long-term stability to 1 part in  $10^8$  but produces a simultaneous reduction of the short-term stability as a consequence. This problem

- 2 -

will be solved by reducing the pressure fluctuations of the temperature controller pump.

The optical system is completed and assembly into a transmitter and receiver unit will start soon. Comparative tests of an AFC loop built at Honeywell and a commercial loop will begin in the middle of February.



## SECTION 2 THE CO<sub>2</sub> LASER

### GENERAL DESIGN

To be of value in a communication system, lasers must fulfill the following requirements:

- High short and long term frequency stability
- Both lasers must be capable of operating by the transition control at one and the same transition of the rotation-vibration band
- Frequency modulation capability
- High-power output in excess of two watts
- Rugged and reliable operation for field application

Two CO<sub>2</sub> lasers were built on the present contract. They represent a further development of the two units delivered on Contract NAS 8-18624. In order to improve the stability, the cavity structure made of Cer-Vit was reinforced to 3 by 3 inches. The cavity length was increased to 14 inches for higher output power, and the heat-decoupled plasma tube was immersed in a temperature controlled water-bath. These changes improved the long-term stability significantly. Both laser mirrors are attached to piezoelectric transducers. One element, a hollow cylinder of K-type lead zirconate/lead titanate, yields, with application of  $\pm 2000$  V, a frequency excursion of 450 MHz. This is in excess of the cavity mode spacing  $c/2l = 428$  MHz and 12 to 14 transitions can be brought into oscillation. One laser, the transmitter, has a piezoelectric element with a cutoff frequency of 2.3 MHz.

The beam is coupled out through the hollow cylinder transducer. A diaphragm between transducer and mirror avoids arc-over problems between discharge and transducer. An Intran 2 mirror with an 85 percent reflecting coating and a radius of curvature of 3m is used as the output coupler. The other mirror is a gold-coated optical flat. Operation in a zero order transverse electromagnetic mode ( $TEM_{00q}$ ) is obtained by insertion of an aperture. Polarization of the beam is achieved by insertion of three wires each having a diameter of 0.0001 inch inside the cavity perpendicular to the beam direction. Figure 1 shows a picture of the disassembled laser. The design of the discharge tube has been simplified, and the active discharge length has increased from 8 to 11.5 inches. Figure 2 shows the assembled laser.

#### PARAMETER TRADEOFF STUDIES

In order to find the optimum operating conditions of the  $CO_2$  laser, a parameter tradeoff study was made. At a given  $Q$  of the cavity (depending on reflectivity of the mirrors and alignment tolerance), the output power depends strongly on parameters such as total pressure, partial pressure of the gas components, excitation current, and total flow rate. In addition, differences exist between the point of maximum power output and the operating point at highest efficiency. The temperature of the discharge tube has a significant influence on the power output.

We have investigated the output of a single-mode, single-frequency  $CO_2$  laser as a function of partial pressure of the gas components, total pressure, gas flow rate and excitation current. The laser was water-cooled by a room temperature water circulating system. The laser was piezoelectrically tuned to oscillate at the P(18) transition which was reported (1) to have the highest power output with an He admixture.

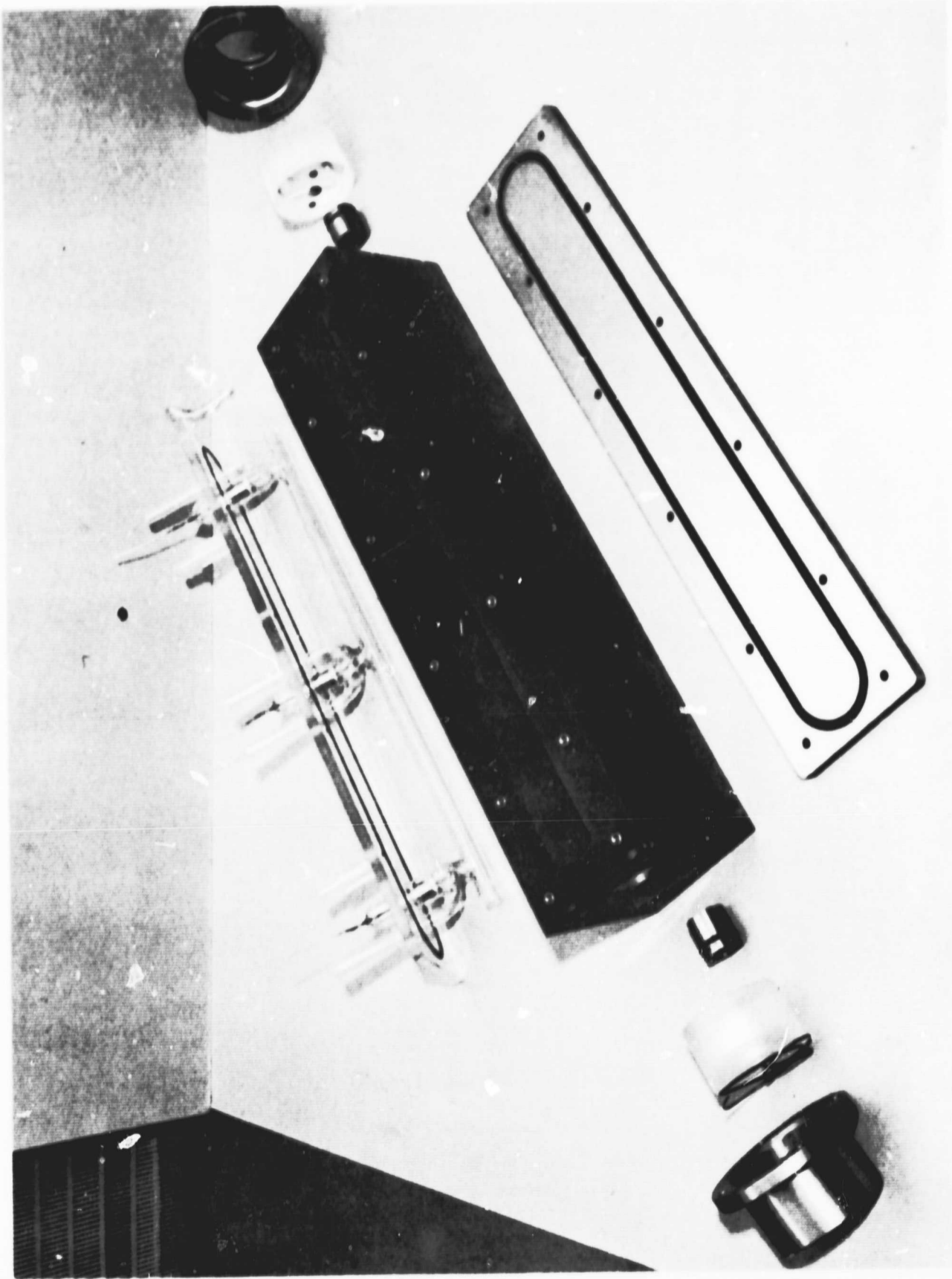


Figure 1. Disassembled View of the Single Mode CO<sub>2</sub> Laser. The quartz cup in the upper right holds the modulation element. The cup in the lower left holds the transition control element.

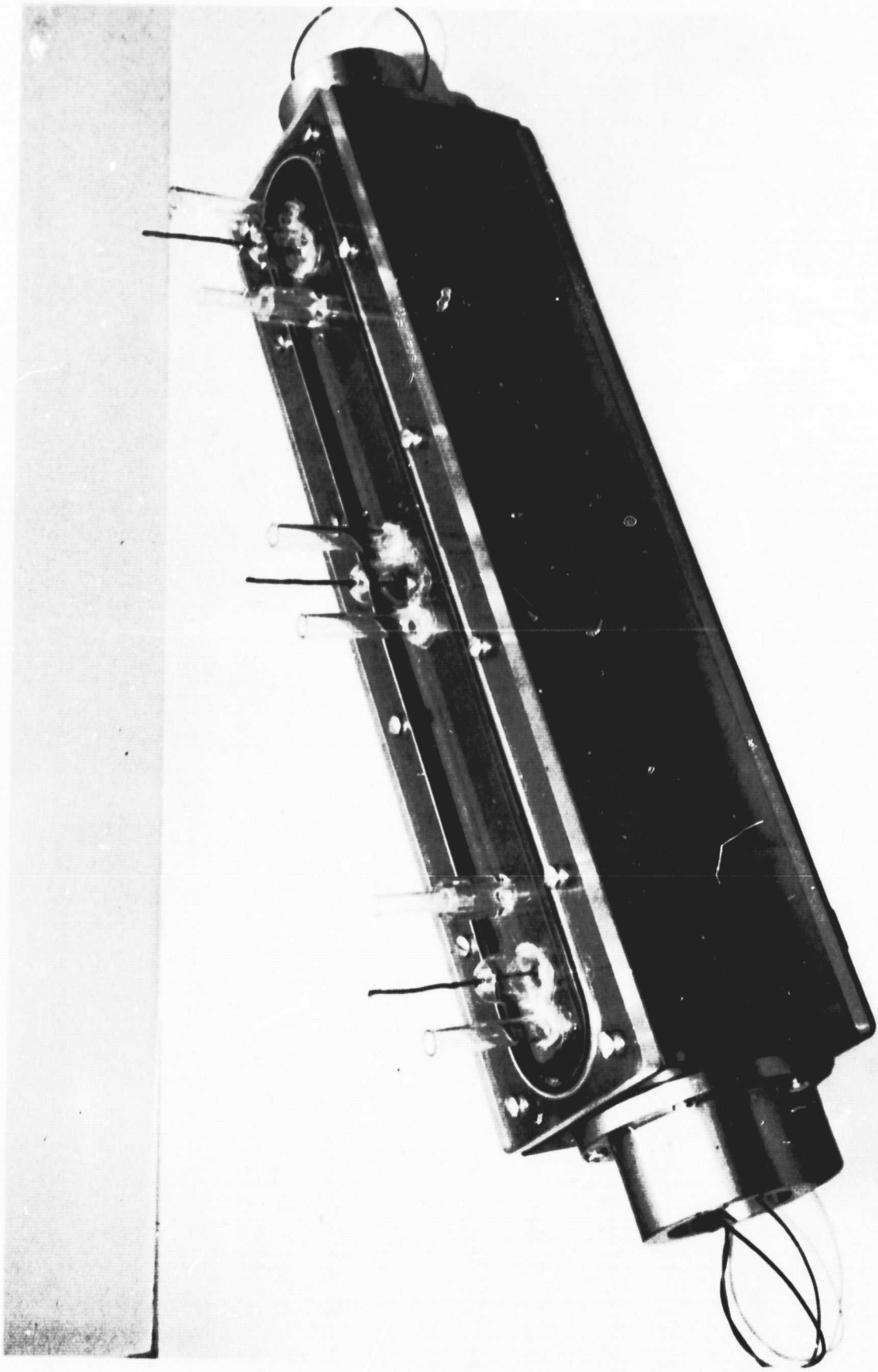


Figure 2. Assembled Water - Cooled Laser

A Coherent Radiation Laboratories power meter (Model 201) was used for power measurement. The pressure was measured at the exit of the tube with a Wallace and Tiernan pressure gauge.

In Figure 3 we have plotted the dependence of the output power as a function of the  $\text{CO}_2$  partial pressure at an absolute pressure of 8 Torr ( $\text{N}_2$  to He ratio = 1:4). The output increases approximately linearly with excitation current and shows a pronounced maximum at approximately 1.1 to 1.2 Torr. The power supply capability was limited to 22.5 mA. The curves, however, indicate that a further increase in excitation would result in a higher output power.

Figure 4 shows the output power as a function of the  $\text{N}_2$  partial pressure at an absolute pressure of 10 Torr ( $\text{CO}_2$  to Helium ratio = 1:4). The  $\text{N}_2$  partial pressure for which the power output is a maximum is a function of the excitation. For large excitation, the maximum is obtained at 2.7 Torr  $\text{N}_2$  partial pressure.

In Figure 5 we have plotted the output power as a function of the He partial pressure at an absolute pressure of 8 Torr ( $\text{CO}_2$  to  $\text{N}_2$  ratio = 1:0.75). Stable operation at a small He content can only be obtained for small excitation currents. For large excitation, the output power increases significantly with increasing He partial pressure and proceeds to a rather flat maximum beyond 4.5 Torr.

The results of the parameter tradeoff study agree with the measurements made by the Raytheon Research Group (2, 3, 4).

These measurements indicate that the optimum gas mixing ratio for highest output power is  $\text{CO}_2:\text{N}_2:\text{He} = 1:2:5$ . For highest power output we operate the laser at 18 to 20 Torr with an excitation of 22.5 mA.

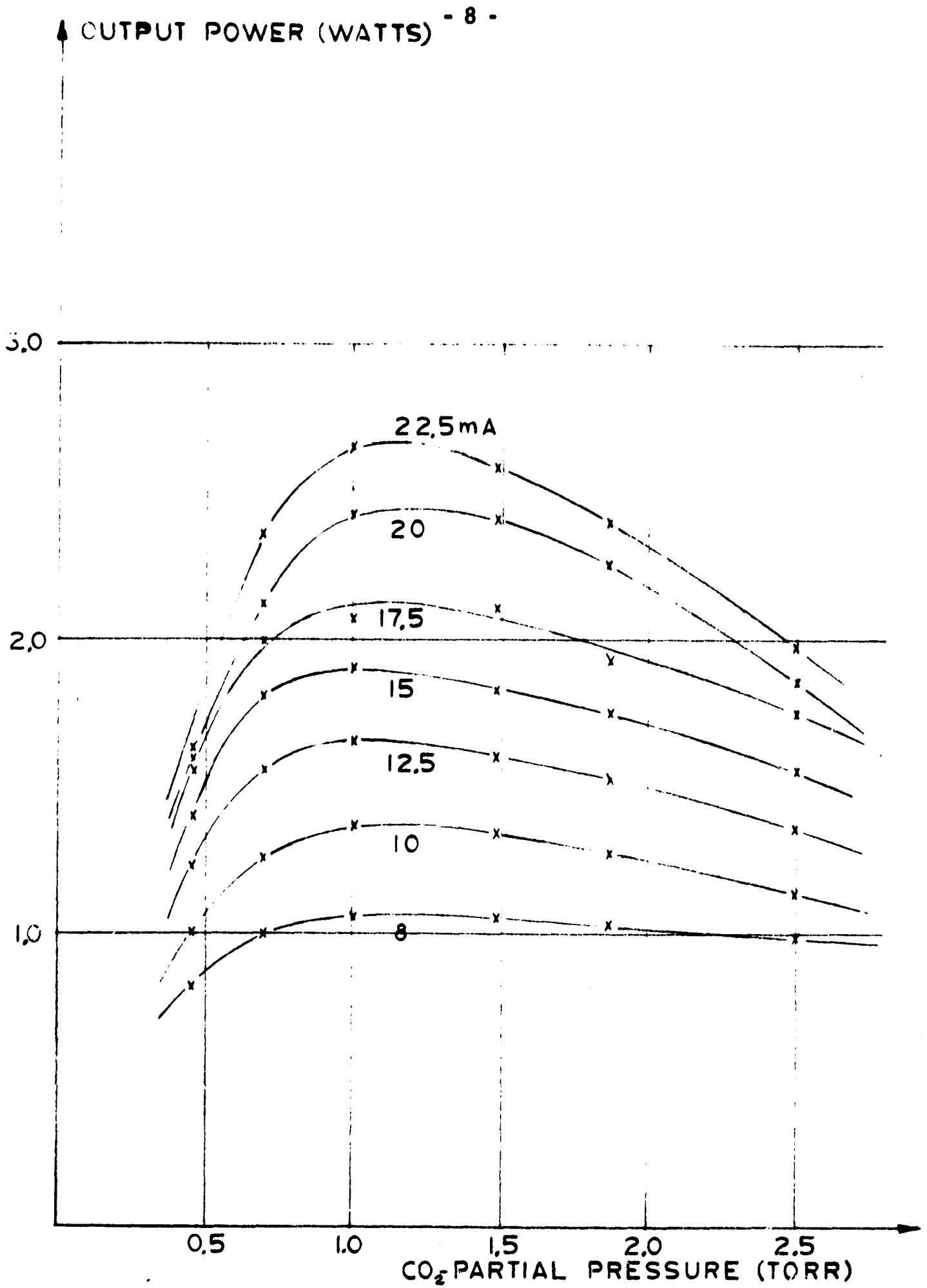


Figure 3. Output Power versus CO<sub>2</sub> Partial Pressure  
 Absolute Pressure = 8 Torr.  
 Nitrogen-to-Helium Ratio 1:4  
 Parameter: Current in mA

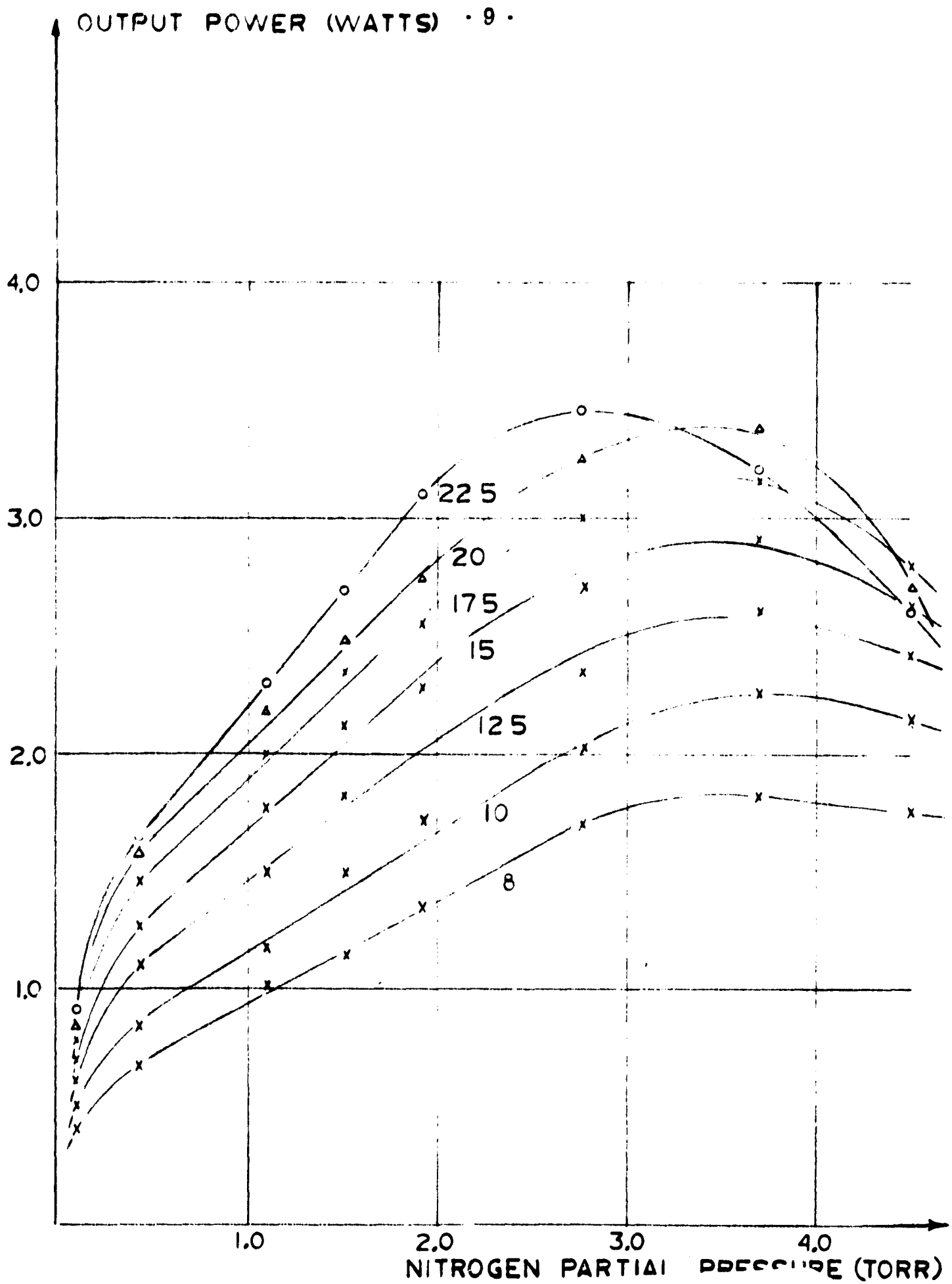
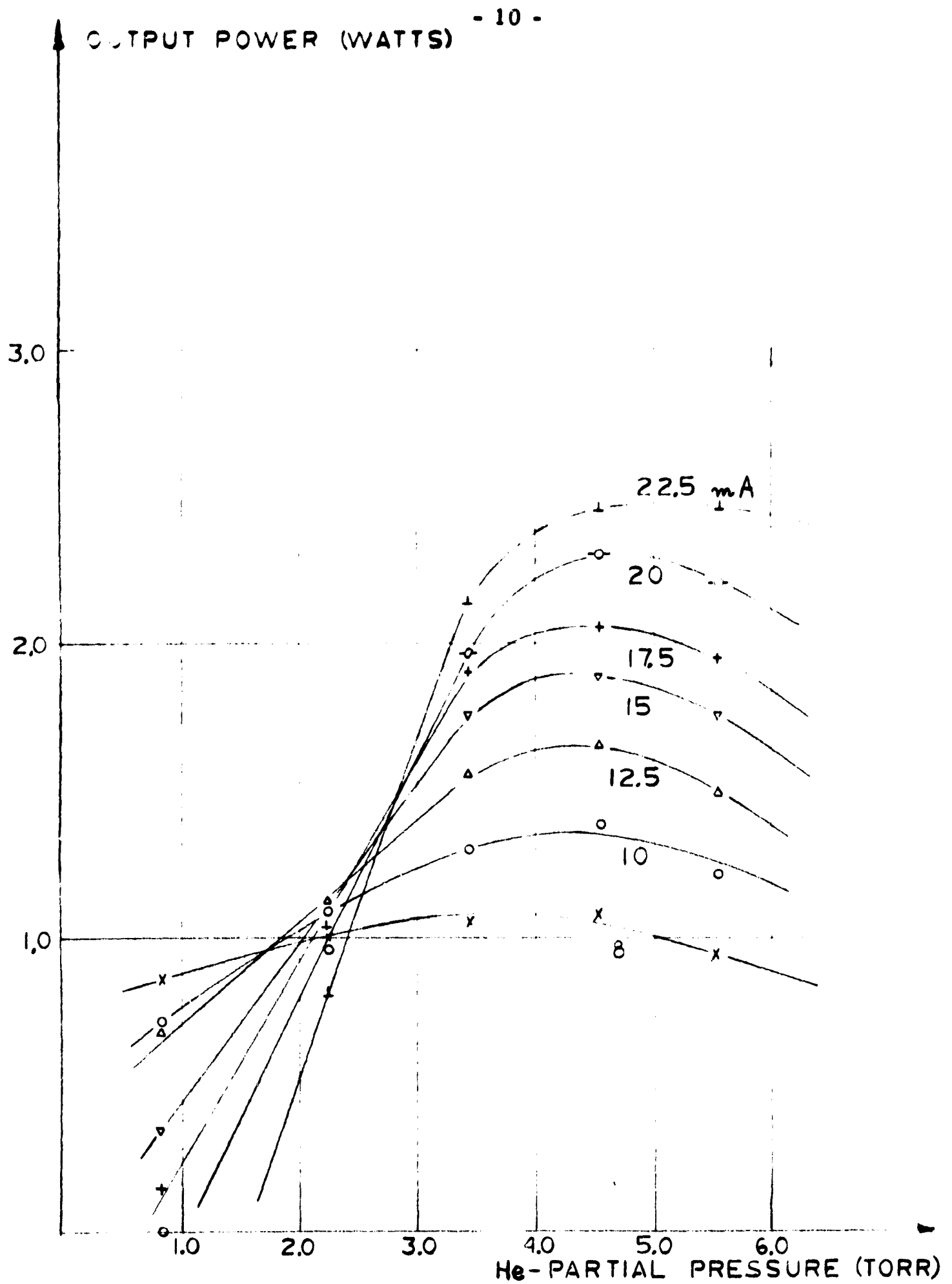


Figure 4. Output Power versus  $N_2$  Partial Pressure  
 Absolute Pressure - 10 Torr.  
 Carbon Dioxide-to-Helium Ratio 1:4  
 Parameter: Current in mA



**Figure 5. Output Power versus Helium Partial Pressure**  
 Absolute Pressure - 10 Torr.  
 Carbon Dioxide-to-Nitrogen Ratio 1:0.75  
 Parameter : Current in mA



The single mode power figures for our laser amount to 18 W/m and the specific power figures to  $0.35 \text{ W/cm}^3$ . They compare favorably with the results reported by other workers (1) in the field.

#### DEPENDENCE OF LASER POWER AND TUBE VOLTAGE ON THE EXCITATION CURRENT

At the optimum gas mixing ratio of  $\text{CO}_2:\text{N}_2:\text{He} = 1:2:5$  we have determined the output power to be a function of the excitation for various absolute pressures. Figure 6 shows the results. The power increases with both increasing excitation and pressure with no sign of saturation. The highest power measured was 4.6 watts at a pressure of 18 Torr with 22.5 mA. excitation. Due to power supply limitation, we were not able to find the saturation region. A further power increase of 20 to 30 percent can be expected for excitations of 30 to 40 mA.

Figure 7 shows the output power for a gas mixing ratio of  $\text{CO}_2:\text{N}_2:\text{He} = 1:1:2$ . The smaller He content is responsible for approximately 50 percent overall power reduction. In addition, for total pressures larger than 15 Torr, saturation with increasing excitation becomes noticeable. This behavior is due to the insufficient depletion rate of the lower laser level.

In Figure 8 we have plotted the tube voltage as a function of the excitation current with the pressure as a parameter. One can recognize that the tube has a negative dynamic resistance which varies between  $12 \text{ k}\Omega$  (at 5 Torr and 20 mA) and  $75 \text{ k}\Omega$  (at 18 Torr and 12.5 mA excitation). With the series impedance of  $100 \text{ k}\Omega$  which was used, the laser can only be operated in a stable condition if the dynamic impedance is smaller than the series impedance. Stable operation at high pressures and small currents is only possible with a large series impedance.

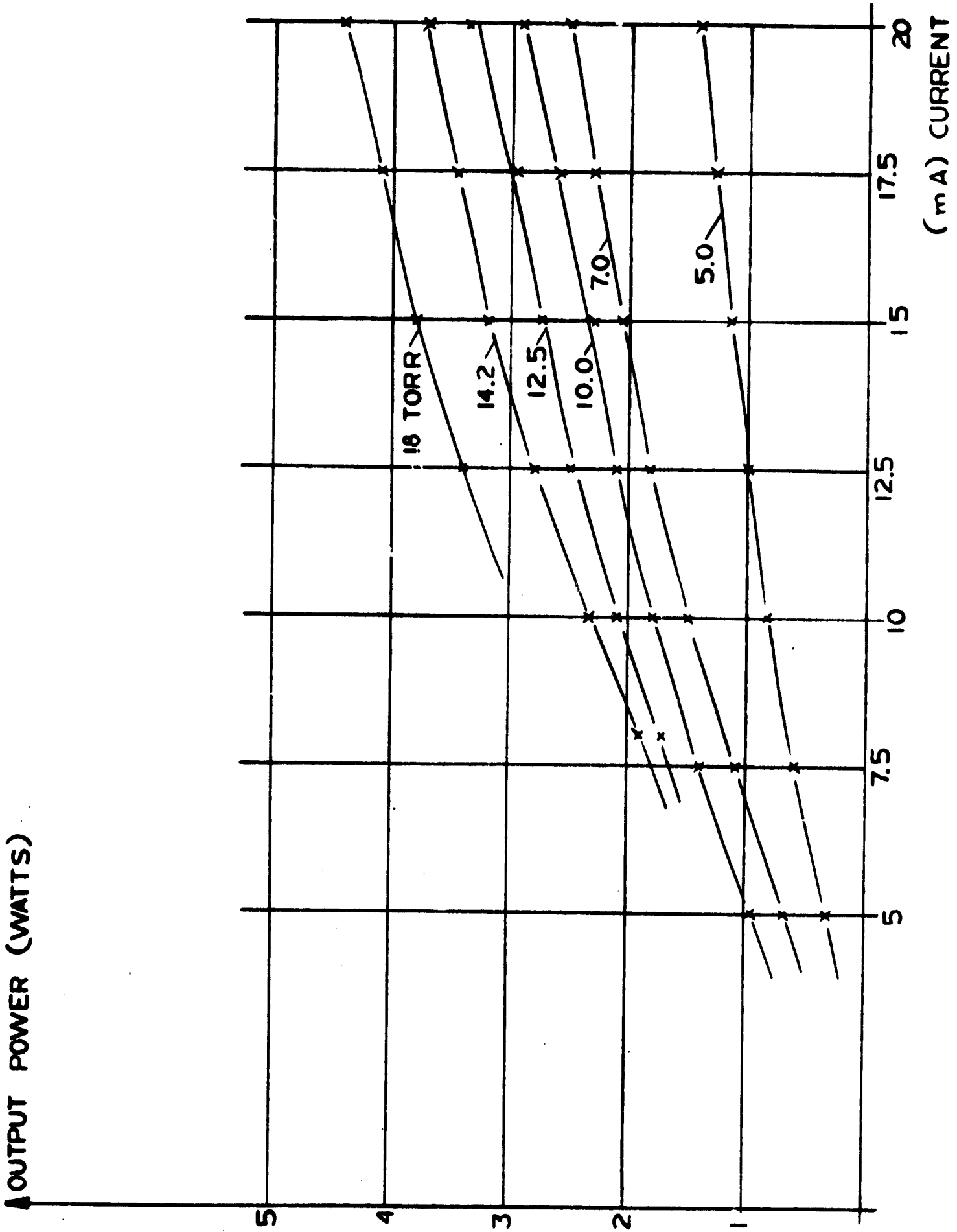


Figure 6. Output Power versus Excitation Current  
Parameter: Operating Pressure (Torr.)  
Gas Mixing Ratio CO<sub>2</sub>:N<sub>2</sub>:He = 1:2:5

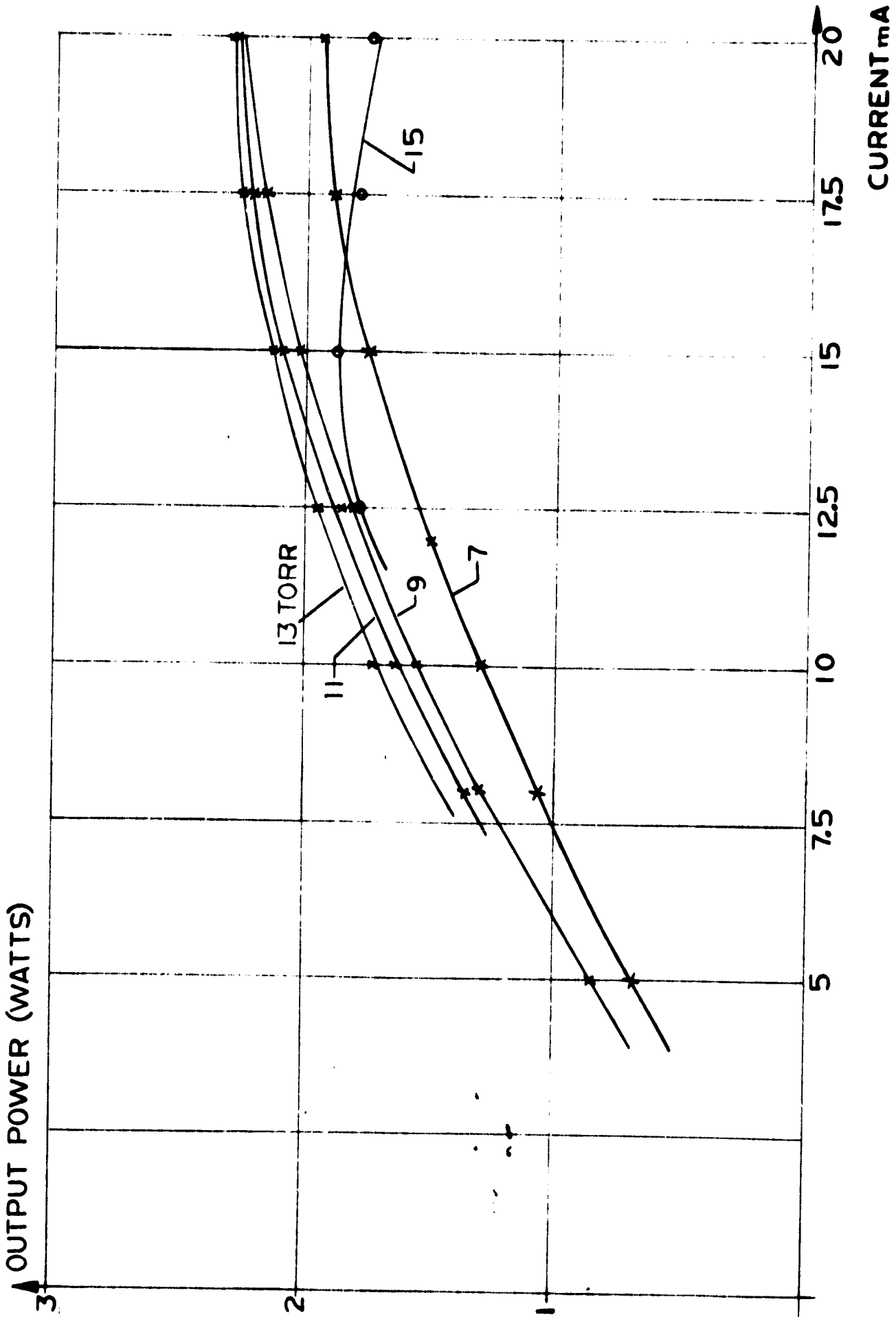


Figure 7. Output Power versus Excitation Current  
Parameter: Operation Pressure (Torr.)  
Gas Mixing Ratio CO<sub>2</sub>:N<sub>2</sub>:He = 1:1:2

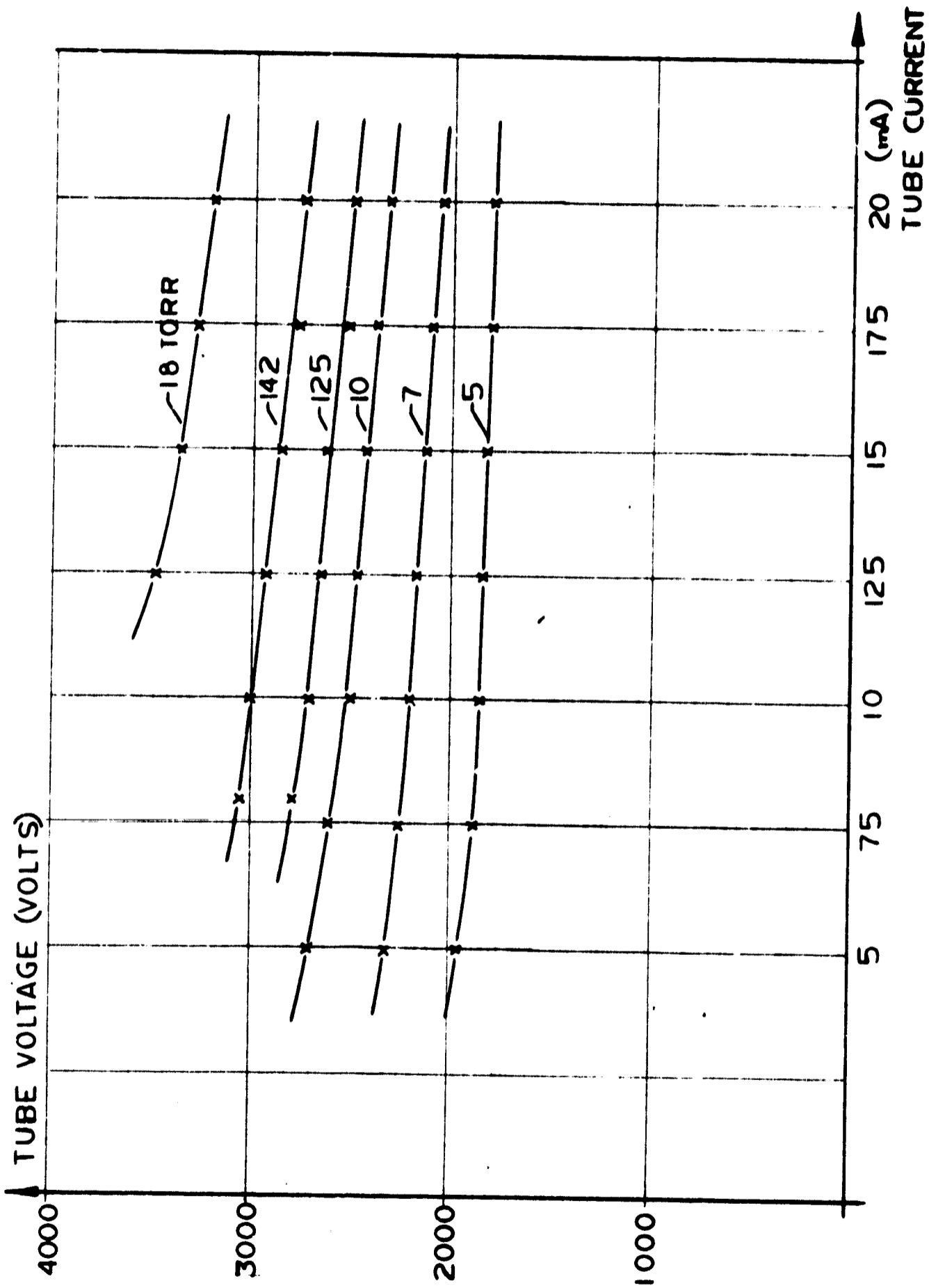


Figure 8. Tube Voltage versus Tube Current  
Parameter: Operating Pressure (Torr.)

We can now calculate the incremental electrical power  $(\Delta V) \cdot I$  that is put into the tube as a function of the excitation current. As characteristic measurements we evaluate those that were taken at an absolute pressure of 10 Torr (approximately 12.5 Torr in the tube). The results are compiled in Table 1 and plotted in Figure 9. As a pronounced effect, we notice that for a small excitation (5 mA.), approximately 63 percent of the excess electrical power is converted into laser power while for a larger excitation (>10 mA.), this percentage levels out to 34 percent or approximately 1/3. This latter value has been found also by Whitehouse et. al. (3). The high percentage at low excitation can be explained by the fact that initially the necessary electron density must be generated by collisions. This conclusion is confirmed by earlier beat frequency shift measurements as a function of excitation. For 5 mA excitation these measurements yielded a shift of 900 kHz/mA., while at a larger excitation of 15 mA the shift reduced to 500 kHz/mA. Thus the incremental electrical power is used to generate and later to maintain the necessary electron density in the discharge.

The laser efficiency in the conversion of electrical input energy into useful laser output energy is strongly dependent upon excitation and pressure. After optimizing the gas-mixing ratio  $\text{CO}_2:\text{N}_2:\text{He} = 1:2:5$ , we have plotted in Figure 10 the efficiency as a function of excitation with the pressure as a parameter. For small currents, the efficiency rises initially until a peak is reached at approximately 10 mA. of excitation. Further increase in excitation reduces the efficiency for all pressures that have been investigated. The highest efficiency that has been reached in single mode operation is 8 percent and is obtained at fairly high pressures only (15-20 Torr). In comparison with Figure 6 we notice that the maximum efficiency is not reached at the highest output power of the laser. An increase in output power beyond 10 mA. has to be paid for by a reduction in efficiency.

A fairly good point of operation both for high efficiency and power output lies at 10 mA. excitation and pressures of 15 to 18 Torr. However, due to the large negative impedance, this point of operation is close to the "drop-out" region of the discharge and good current control is required.

Table I. Incremental Electrical Power

Excitation (mA)	5	7.5	10	12.5	15	17.5	20
Incremental Electrical Power $W_1$ (Watts)	0.60	0.64	0.61	0.64	0.765	0.893	1.02
Laser Power $W_2$ (Watts)	0.95	1.4	1.8	2.1	2.3	2.6	2.9
$\epsilon = \frac{W_1}{W_2}$	0.63	0.46	0.34	0.305	0.332	0.344	0.352

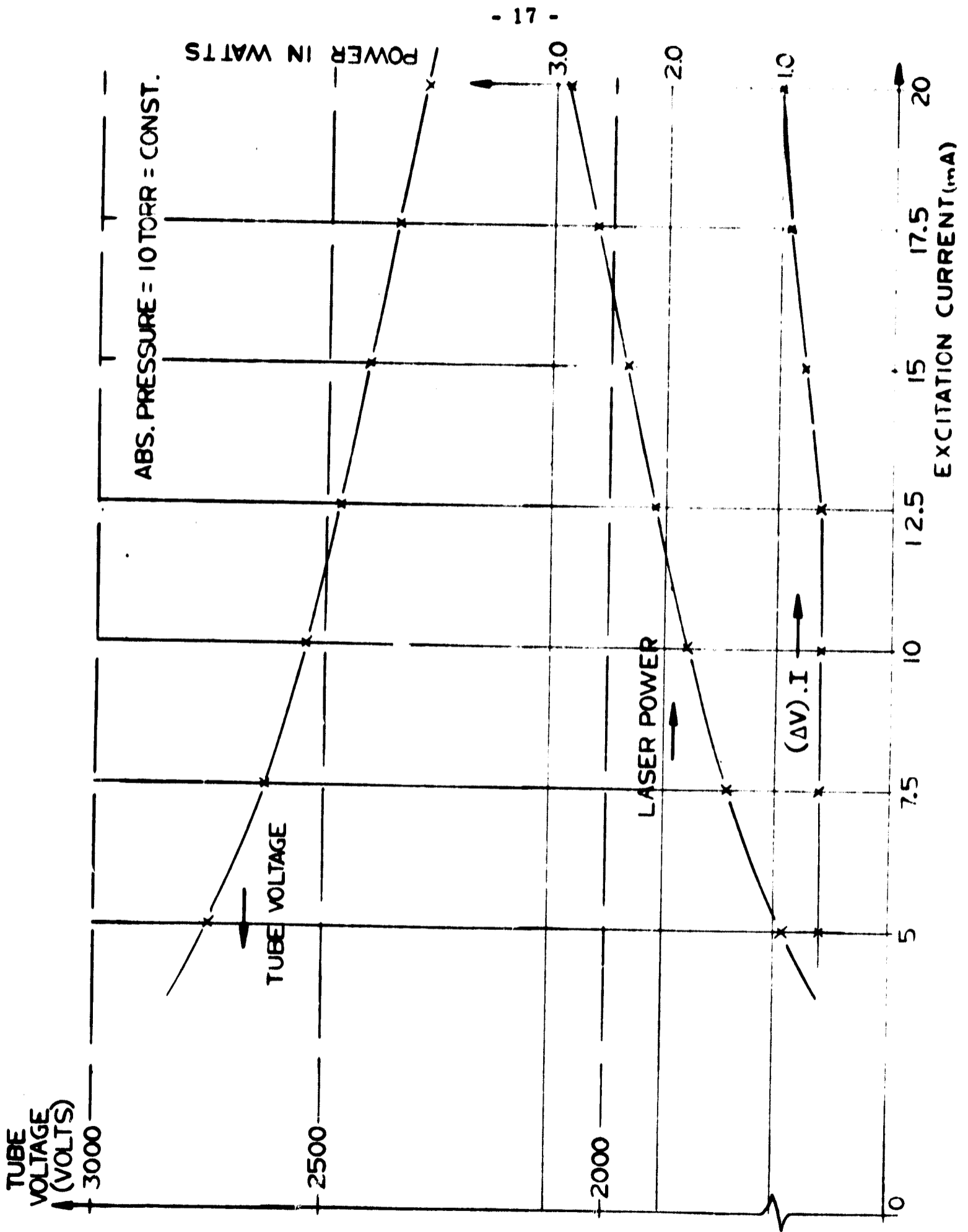


Figure 9. Tube Voltage, Laser Power and Incremental Electrical Power versus Excitation Current

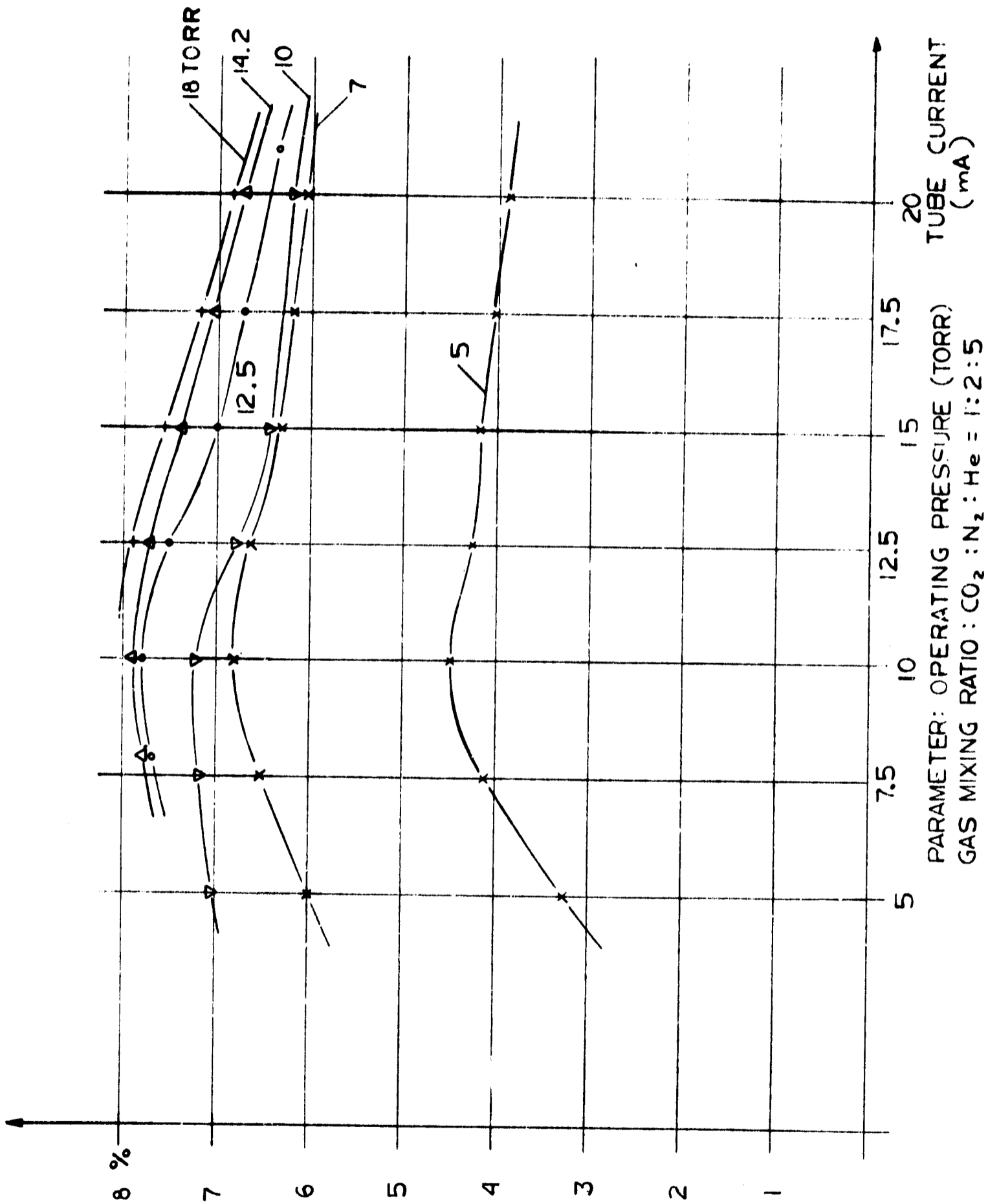


Figure 10. Single Mode Efficiency versus Excitation Current



In multi-mode operation the efficiency is at least twice as large or 16 percent, possibly up to 20 percent. Both the single mode and multi-mode efficiencies compare favorably with results obtained by other workers in the field.

### LASER BEAM SPREAD AND AMPLITUDE STABILITY

Previous proof of single-mode operation was based on obtaining a single circular spot on heat-sensitive wax paper. In order to provide more conclusive evidence of single mode operation, we have measured the beam spread of the laser in the far-field. The experimental setup shown in Figure 11 was used.

In operation of the test setup a Barnes thermistor bolometer with a 2x2 mm sensitive area is mounted on a two-dimensional positioner 4.5 m from the laser. A chopper and a lock-in amplifier (PAR) are used for detection. A recorder was used for the amplitude stability measurements.

The laser is operated from a non-regulated dc power supply. The flowing gas supply is provided by a set of CO<sub>2</sub> - N<sub>2</sub> - He bottles and a vacuum pump. No effort was made to flow-stabilize the laser. Cooling is provided by a water-circulator (Lear-Siegler) without temperature control.

Figure 12 shows the laser intensity as a function of distance at a 4.5 m separation of detector from the laser. A typical gaussian intensity distribution was obtained to distances where the intensity was reduced by 4 orders of magnitude from the beam center intensity. The measured beam-spread at the half-power point is 2.4 milliradians. The theoretical limit imposed by diffraction theory ( $\theta = 1.22 \frac{\lambda}{d}$ ) is 2.3 m rad. It is therefore justified to say that the CO<sub>2</sub> laser is diffraction-limited and that an improvement in spatial power density (watts/steradians) can only be obtained by increasing the power level of the laser.

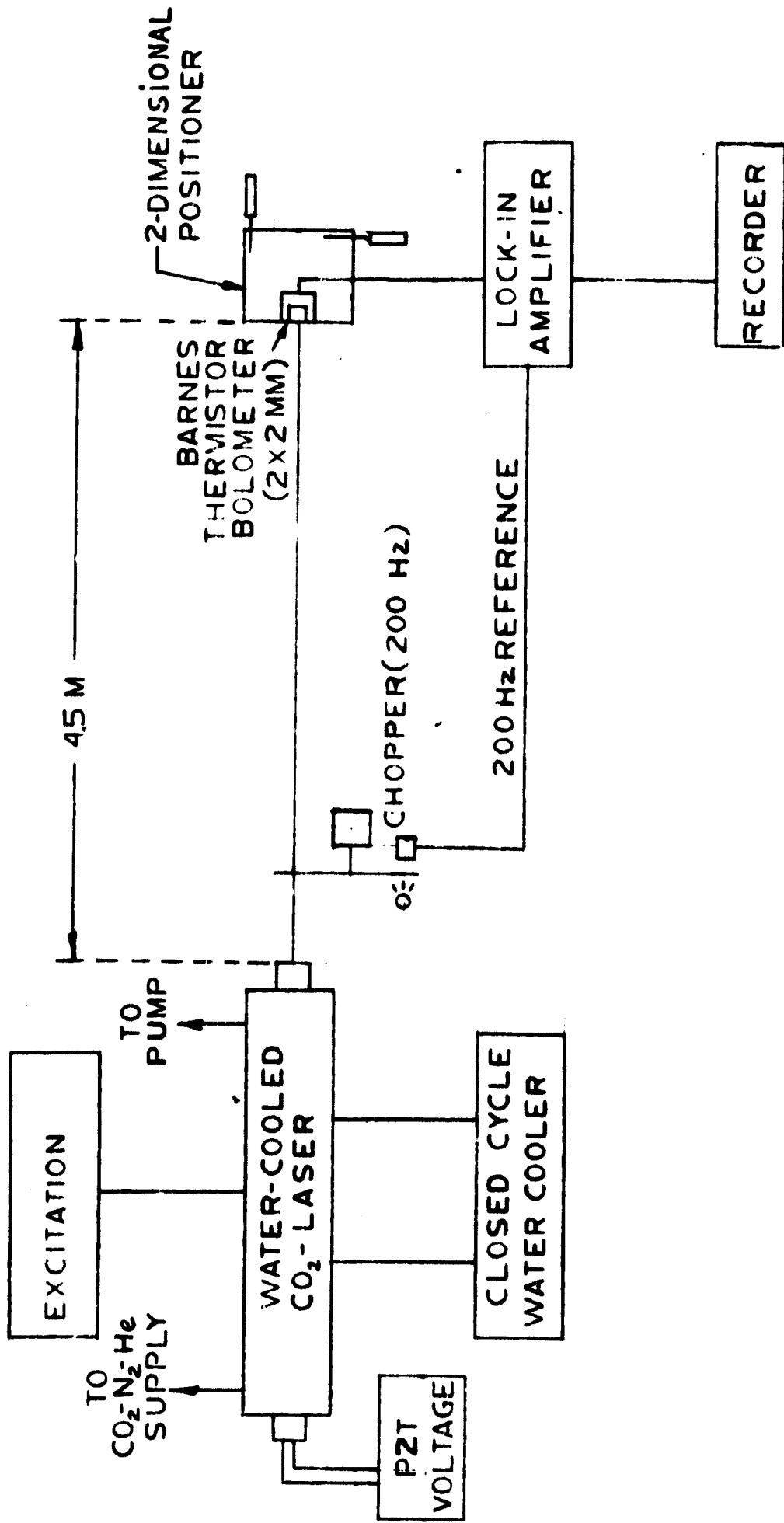


Figure 11. Experimental Setup to Determine Beam Spread and Amplitude Stability

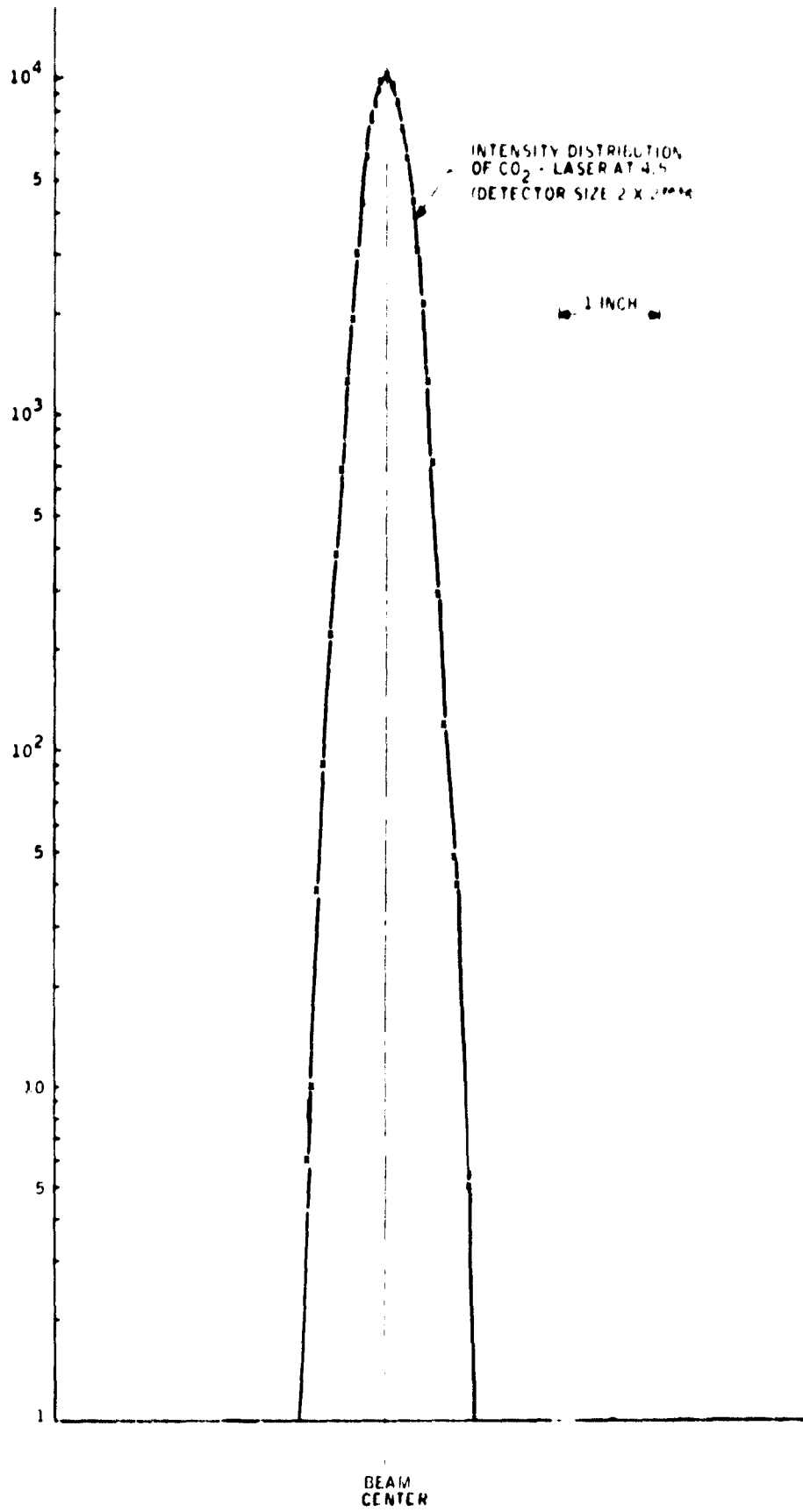


Figure 12. Intensity Distribution of CO<sub>2</sub> Laser

With the thermistor detector aligned at the beam center, we have recorded the laser intensity over time periods up to 3 hrs. Figures 13 and 14 show typical records of the laser intensity for two piezoelectric voltage settings. The intensity fluctuations over a three hour period are generally within  $\pm 2$  percent. Under certain operating conditions (operation at doppler center of a strong transition) the stability over time intervals of 40 min was  $\pm 0.5$  percent (see Figure 13b). As a result of these measurements it can be said that by proper placement of a cavity mode at a strong transition, the amplitude stability over periods of 1 hour is within  $\pm 1$  percent.

## LASER FREQUENCY CHARACTERISTICS

Spectral measurements of both lasers were made with a Perkin-Elmer 99 G spectrometer as a function of the piezoelectric tuning voltage. A thermistor detector was used at the exit slit of the spectrometer. Improvement in spectral resolution was obtained by using the spectrometer in the double-pass configuration. A re-calibration with the He-Ne 6328Å laser was necessary.

The hollow cylinder PZT transducer exhibited a frequency throw of 450 MHz which is sufficient to overcome the axial mode spacing until a consecutive transition starts to oscillate. The piezoelectric sensitivity was measured, and amounts to 110 kHz/volt for the transition control element. Table II shows all transitions that have been found to oscillate in both lasers at optimum mixing ratio, 10 Torr pressure and 10 mA excitation. In the table we find also the frequency width of oscillation measured between half-power points. We notice that the stronger transitions from P(16) to P(22) show also the largest frequency width of oscillation which lies anywhere between 33 and 71 MHz. This is important since both lasers are setoff by 10 MHz and sufficient tracking range due to temperature fluctuations must be allowed for both the high and low frequency side of the spectrum. In an earlier report we have postulated that both lasers should have a width of oscillation of

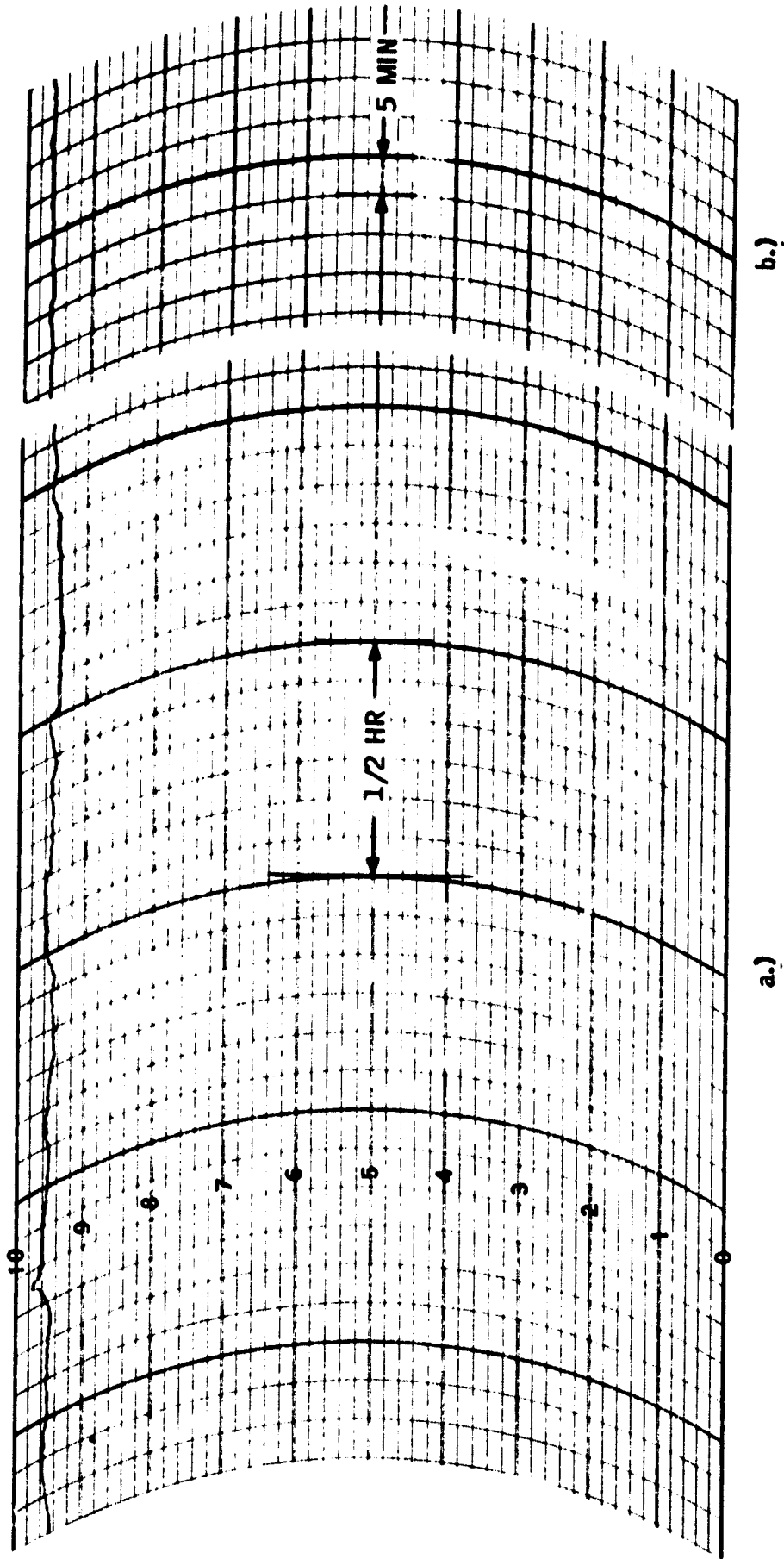


Figure 13. Amplitude Stability Measurement  
(a) 1500v PZT Voltage, 2 1/2 Hr Time Span  
(b) 550v PZT Voltage, 40 Min Time Span

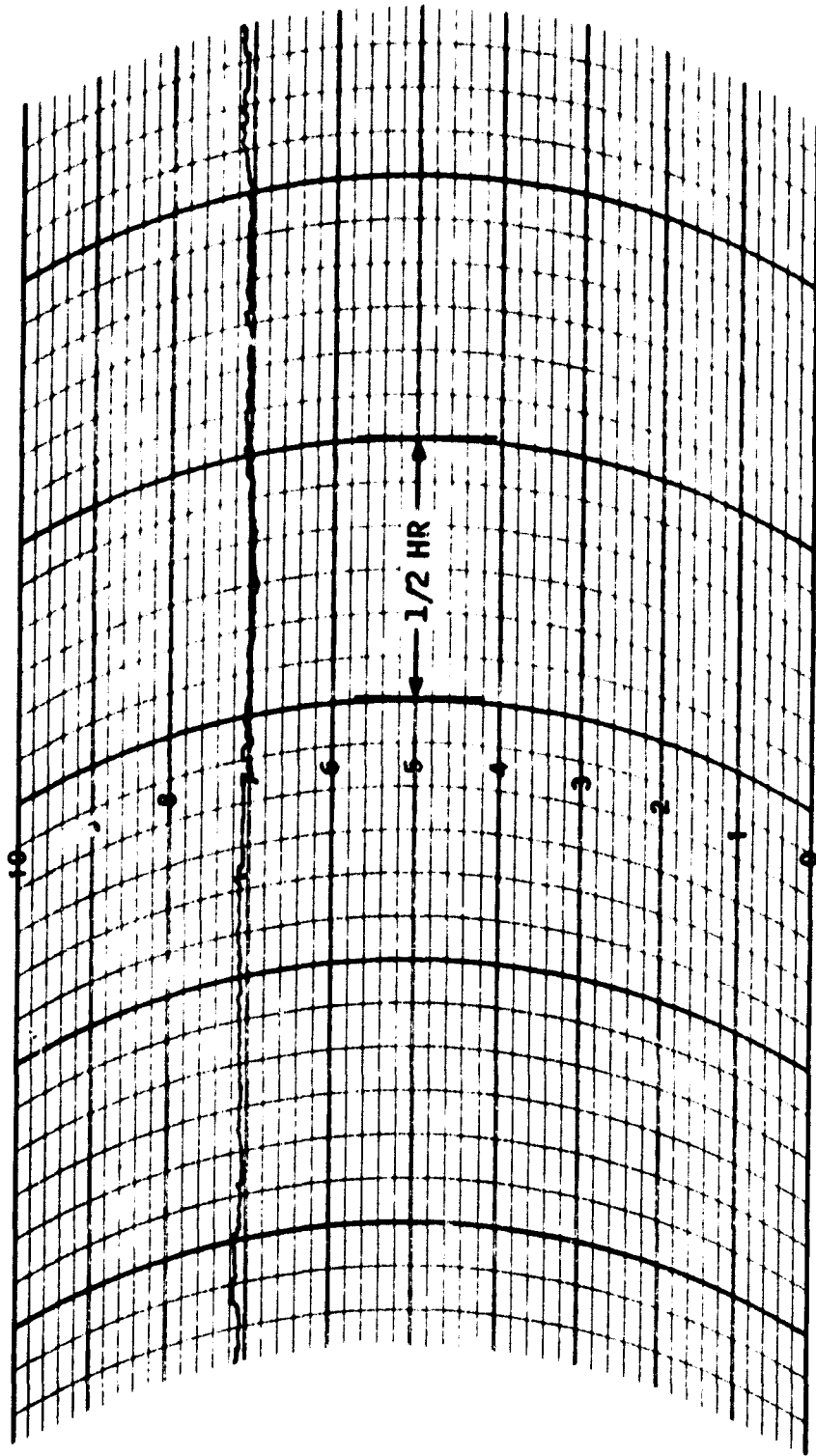


Figure 14. Amplitude Stability Measurement  
200 v PZT Voltage, 2 1/2 Hr Time Span

Table II. Transitions Under Oscillation in Laser 1 and 2  
(from -2000 to 0 to 2000 PZT Voltage = Axial  
Mode Spacing = 428 MHz).

	Transition	$\lambda$ Measured	$\lambda^*$ Reference	Width of Oscillation (MHz)
Laser 1	P(14)	10.530 $\mu$	10.5326 $\mu$	44
	P(22)	10.608	10.6118	55
	P(30)	10.694	10.6965	10
	R(12)	10.301	10.302 *	10
	P(12)	10.512	10.5135	31
	P(16)	10.550	10.5518	71
	P(20)	10.589	10.5912	55
	P(24)	10.629	10.6324	5
	P(18)	10.569	10.5713	33
	P(26)	10.650	10.6534	22
	R(20)	10.242	10.246 *	12
	R(14)	10.286	10.288 *	35
Laser 2	R(18)	10.255 $\mu$	10.259 * $\mu$	11
	P(24)	10.629	10.6324	33
	P(12)	10.512	10.5135	15
	R(24)	10.215	10.219 *	22
	P(26)	10.650	10.6534	32
	R(14)	10.286	10.288 *	33
	P(16)	10.550	10.5518	44
	P(22)	10.608	10.6118	35
	R(22)	10.232	10.233 *	39
	P(18)	10.569	10.5713	55
	P(20)	10.589	10.5912	42
	R(20)	10.242	10.246 *	10
	P(14)	10.530	10.5326	32

\*Note: The wavelength is measured and identified by Patel (5), those marked with an asterisk by Howe (6)

± 25 MHz. From Table II we see that the transitions from P(14) to P(22) do fulfill this requirement. The following pairs do not fulfill this requirement (disqualification of one transition in one laser disqualifies the pair): P transitions P(12), P(24), P(26), P(30).

None of the R-line pairs qualify with the exception of R(14). R-line transition however should be discarded since its appearance is closely related to the gain of the system and therefore dependent on the gas mixing ratio and pressure in the laser. In addition many R-transitions in one laser do not appear in the other laser.

The relative laser intensity in each transition as it appears at the output of the spectrometer was measured as a function of the piezoelectric voltage. Figure 15 and 16 show such a scan for a pressure of 10 Torr and 10 mA excitation for lasers 1 and 2. In Figures 17 and 18 the same type of scan is made for a pressure of 5 Torr and 7.5 mA excitation.

Most interesting to note is that the appearance of the transitions as a function of the applied voltage occurs in a more statistical fashion and shows no correlation between the two lasers. Although both laser cavities are equal, within a tolerance  $5 \times 10^{-3}$  cm, this tolerance is not close enough to make a transition appear in either laser at the same voltage setting. It is estimated that the length tolerance would have to be  $\pm \frac{\lambda}{m} \approx 1\mu$  where  $\lambda$  = wavelength and  $m$  = number of transitions under oscillation over  $\Delta V_c$ . Machining to a tolerance of 1 micron at a 35 cm cavity length is not feasible at this time. Matching of a pair of transitions of two lasers is only achievable at present by piezoelectric frequency control in form of a d.c. bias on the transition control element.

It is important to note that both lasers oscillate over most of the frequency spectrum in single frequency operation. Especially, all strong P transitions that qualify for heterodyning purposes oscillate one at a time. Multi-frequency oscillation can occur only during narrow portions of the spectrum when weak P or R transitions are free to oscillate. These portions of the spectrum must be avoided in order not to throw off the AFC loop from tracking the transmitter laser.



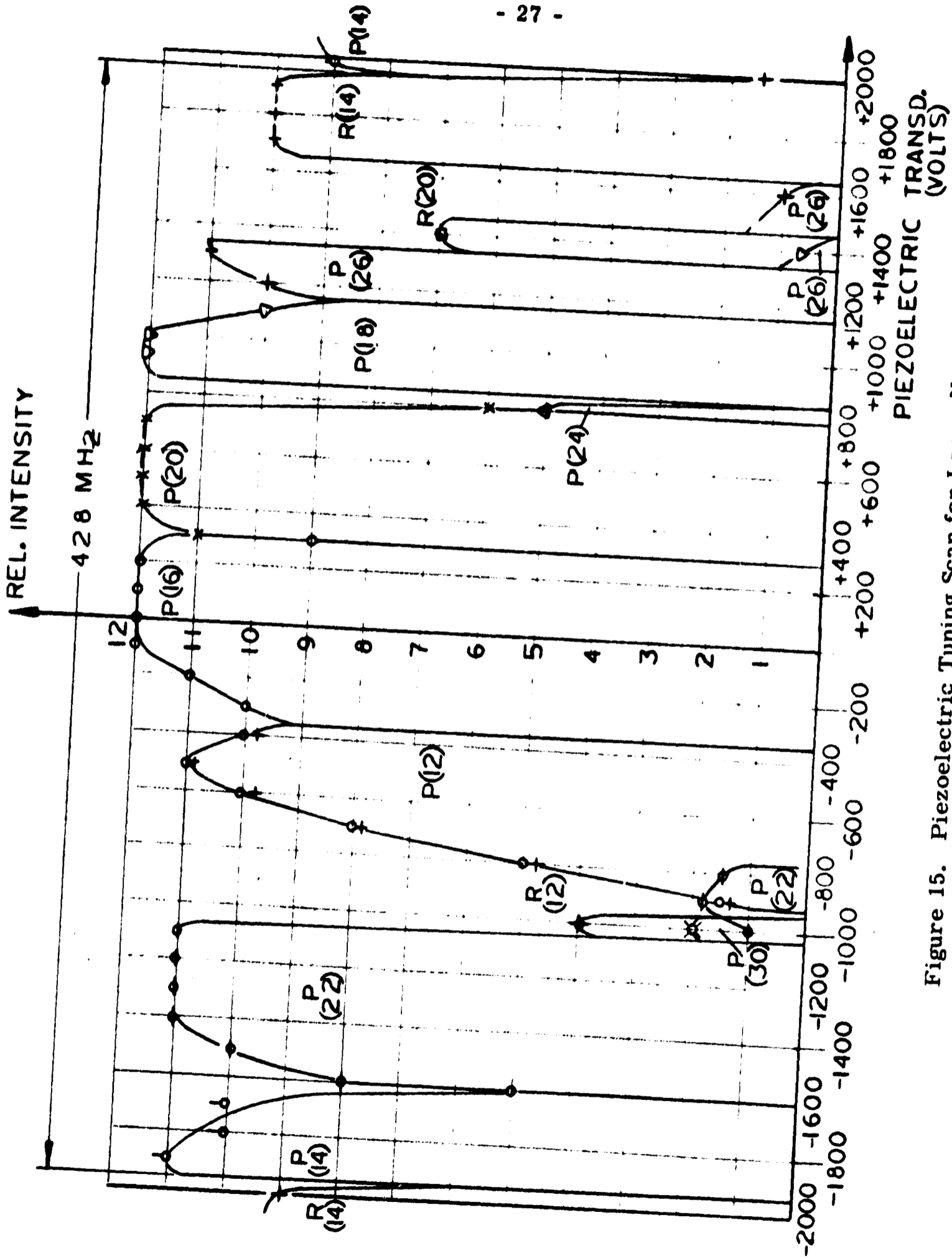


Figure 15. Piezoelectric Tuning Scan for Laser No. 1  
P = 10.0 Torr.  
I = 10 mA

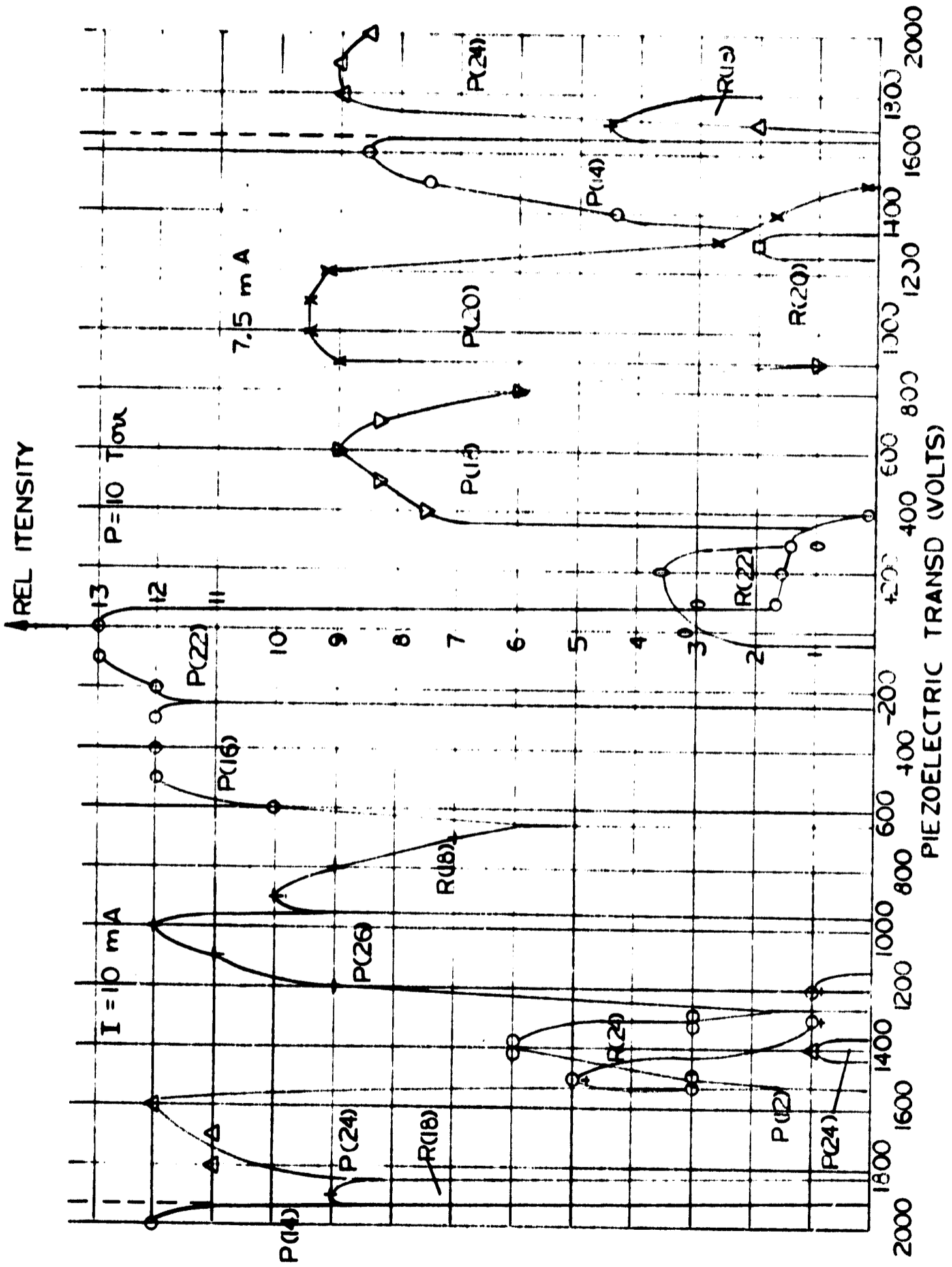


Figure 16. Piezoelectric Tuning Scan for Laser No. 2  
 P = 10.00 Torr.  
 I = 10 mA

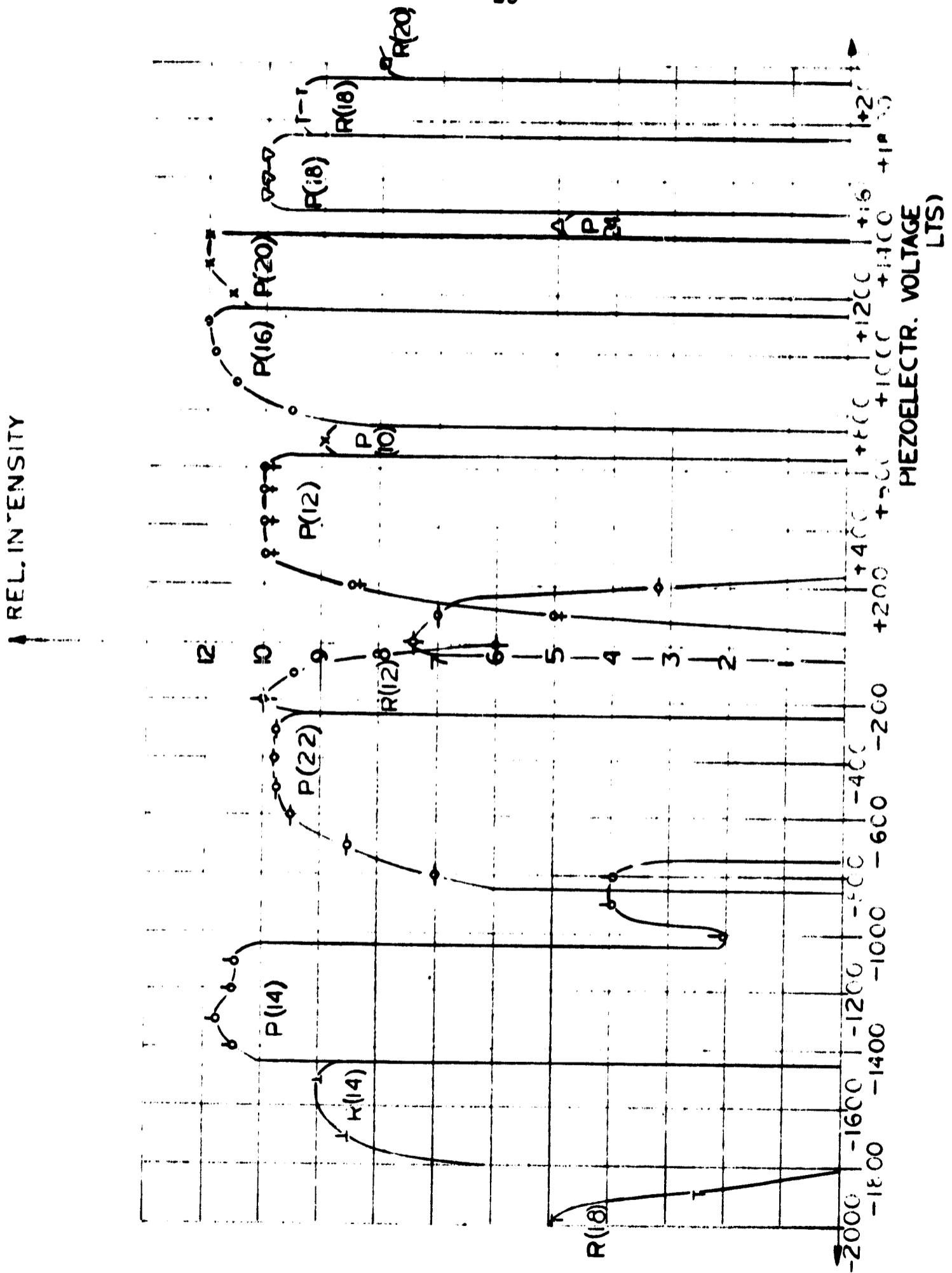


Figure 17. Piezoelectric Tuning Scan for Laser No. 1  
P = 5.0 Torr.  
I = 7.5 mA

↑ REL. INTENSITY

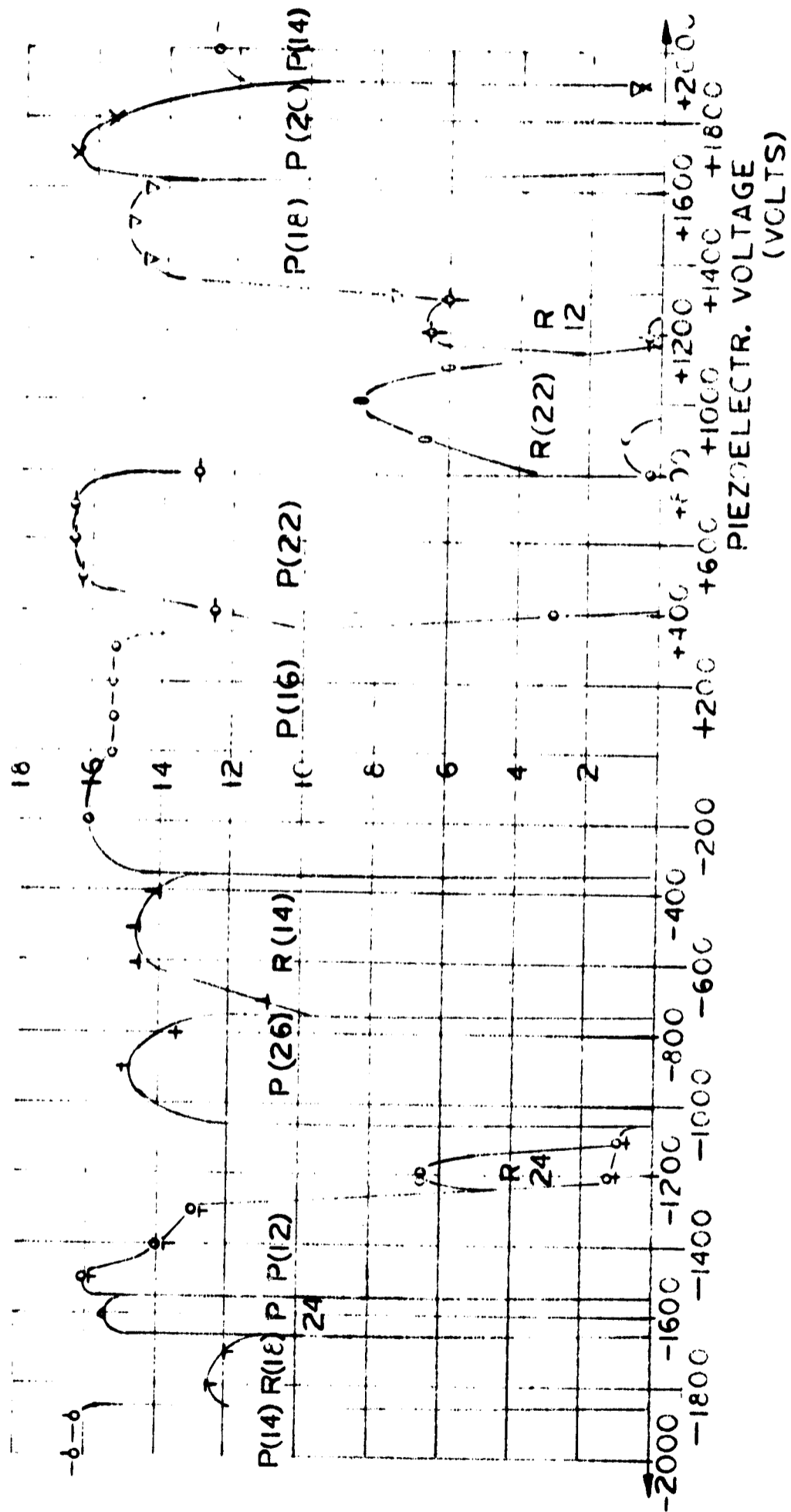


Figure 18. Piezoelectric Tuning Scan for Laser No. 2  
P = 5.0 Torr.  
I = 7.5 mA

Although the intensity in one transition will cease abruptly at the point of transition exchange, the total intensity as measured with a bolometer shows only smaller variations over the piezoelectric tuning range. Figure 19 shows a tuning scan made with a motor-driven high voltage potentiometer between 0 and 2000 V with linearly increasing and decreasing voltage at 5 Torr pressure and 5 mA excitation.

From Figure 19 we can recognize a high repeatability of the "backwards" scan (2000 V  $\rightarrow$  0) with the "forward" scan (0  $\rightarrow$  2000 V) but a pronounced hysteresis effect is noticeable.

The hysteresis could be largely reduced by shunting the PZT element with a 100 k $\Omega$  resistor. Figure 20 shows a manual tuning scan at a pressure of 10 Torr and 10 mA excitation. Some hysteresis however is connected with the laser mechanism and affects the spectrum such that a transition under oscillation remains under oscillation. Effects of this type have also been found in reactive Q-switched CO<sub>2</sub> lasers (7) where one cavity mirror was moved at a rather rapid rate.

**FOLDOUT FRAME |**

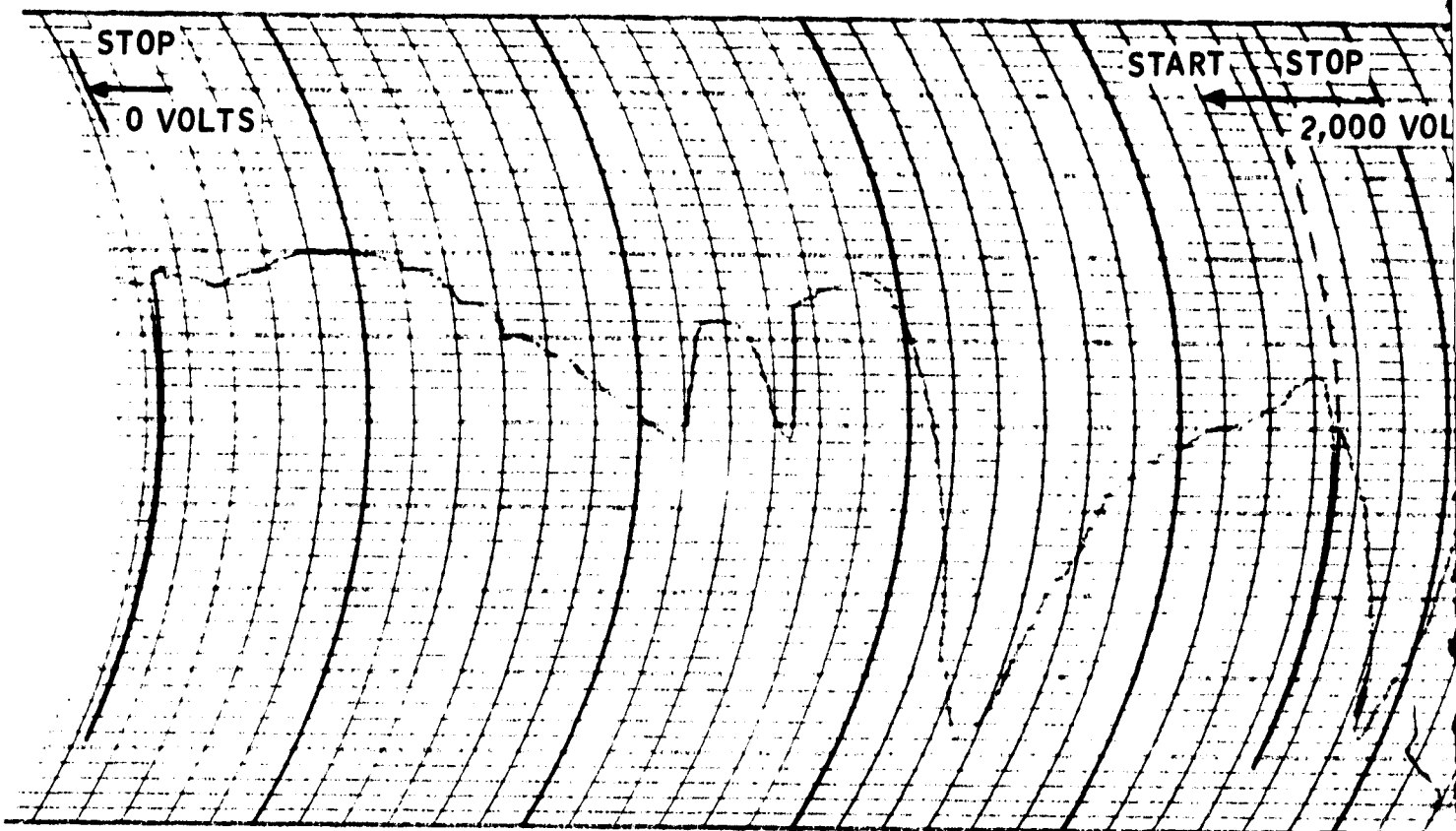
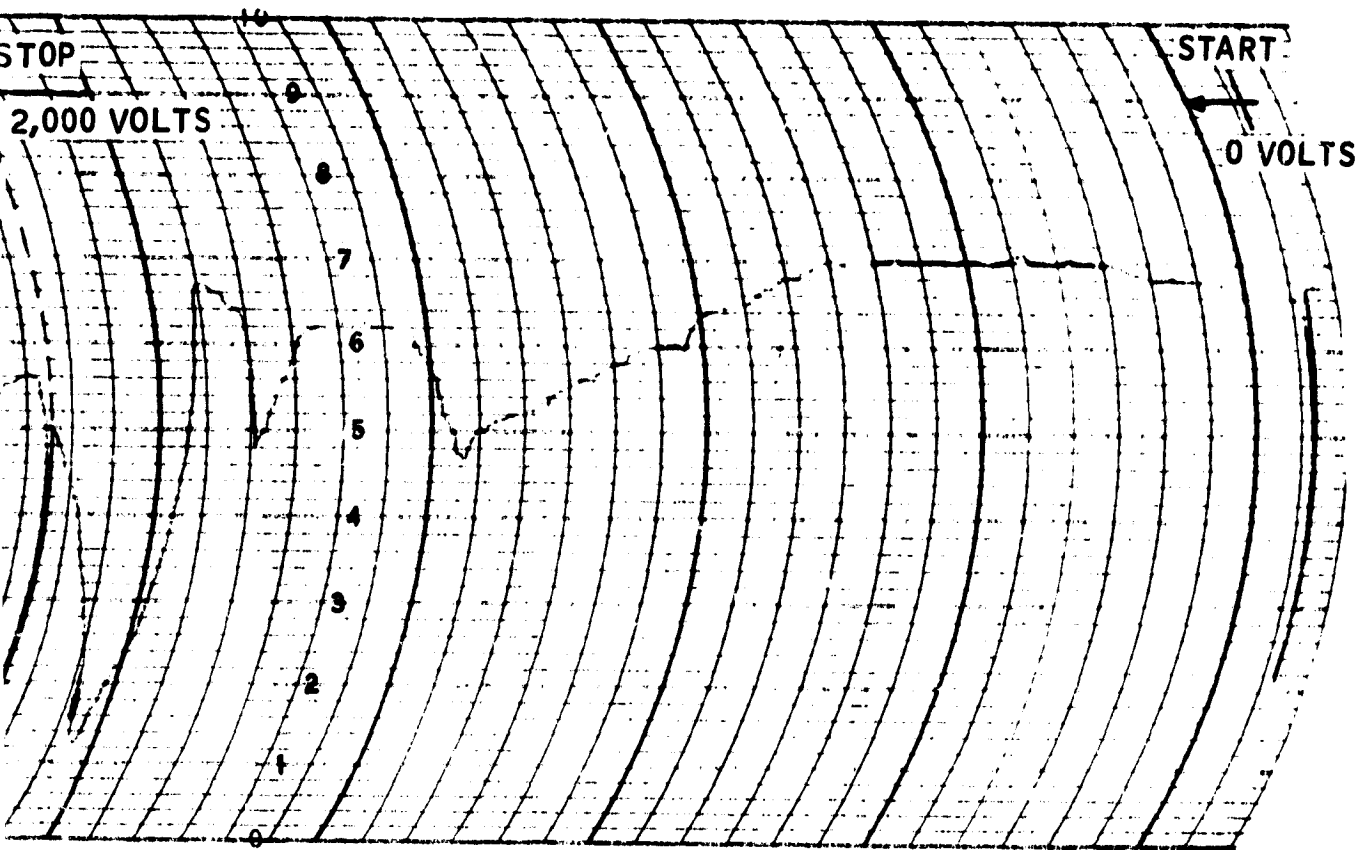


Figure 19. Piezoelectric Tuning S  
CO<sub>2</sub> Laser



Tuning Scan of Single Mode

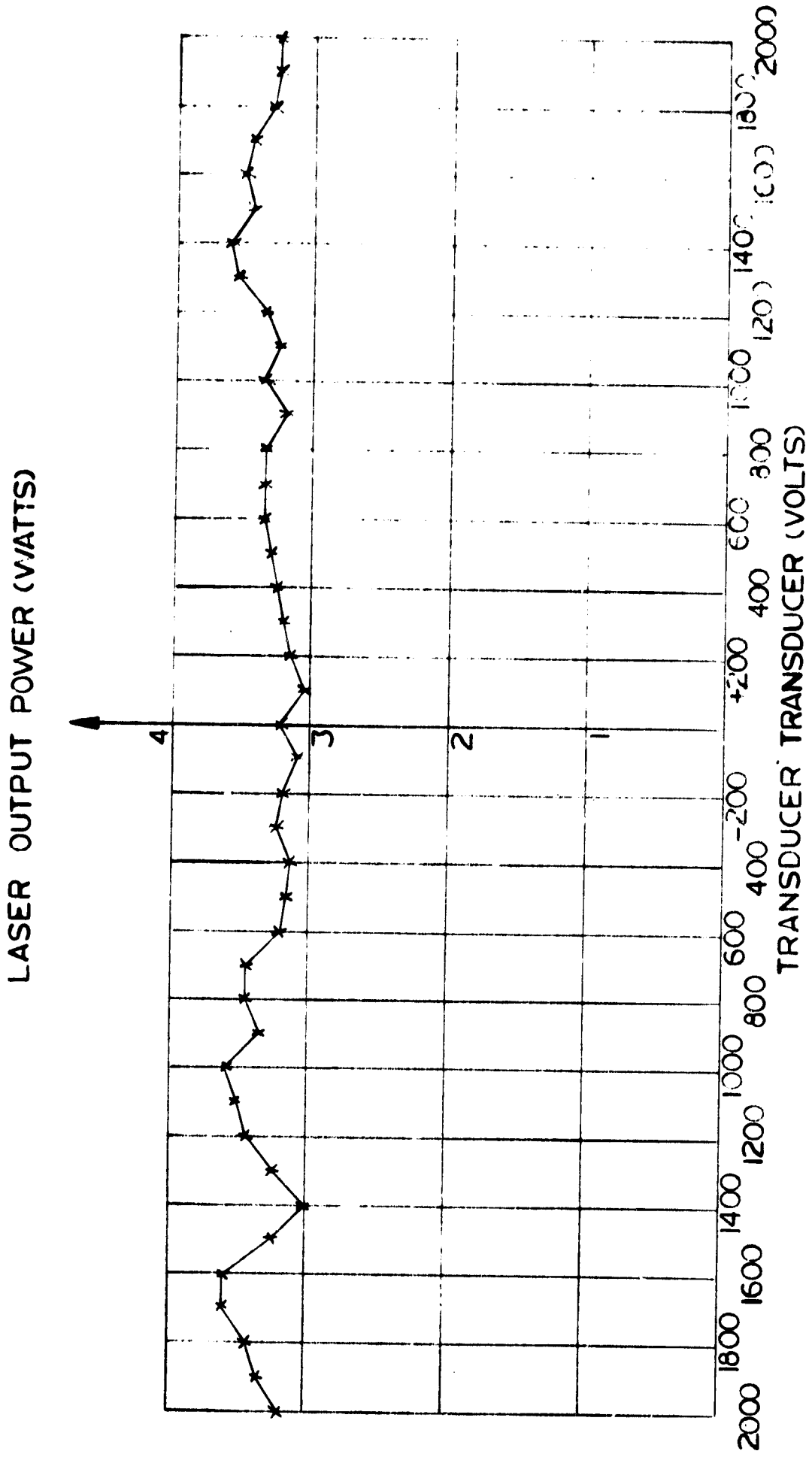


Figure 20. Single Mode Laser Power versus Piezoelectric Voltage Setting



### SECTION 3 OPTICAL HETERODYNE EXPERIMENTS

The CO<sub>2</sub> lasers were heterodyned on the surface of a liquid-nitrogen-cooled HgCdTe detector. The experimental setup is shown in Figure 21 and has only minor modifications in comparison to the system that was used in previous heterodyne experiments. The simultaneous use of the spectrometer turned out to be useful. It obtains energy from laser 1 on reflection, and from laser 2 by transmission through the germanium beam combiner. Both lasers were cooled with a water-recirculating system (Type Lear-Siegler) without temperature control. For the communication system each laser will be independently controlled by a Lauda temperature controller which has an accuracy of  $\pm 0.01^\circ\text{C}$ .

Piezoelectric frequency control is provided by two Fluke Power Supplies (0.001 percent voltage regulation). The relative stability was measured with a Panoramic Spectrum Analyzer and an oscilloscope. Early observation of the beat frequency fluctuations could be traced to flow fluctuations in the discharge path similar to a fluid oscillator. In order to avoid those fluctuations, both flow inlets of the laser were fed from one buffer volume.

Figure 22 shows a photograph of the heterodyne set-up mounted on the three-ton granite slab.

#### BEAT FREQUENCY CHARACTERISTICS

The opportunity to select any desired transition for both lasers was a useful factor in obtaining the heterodyne beat signal. Beats on the transitions from P(16) to P(22) were obtained by applying the required bias voltage according to Figures 15 to 18 on the corresponding transition control element. The long-term stability for both lasers, even when operated without cooling

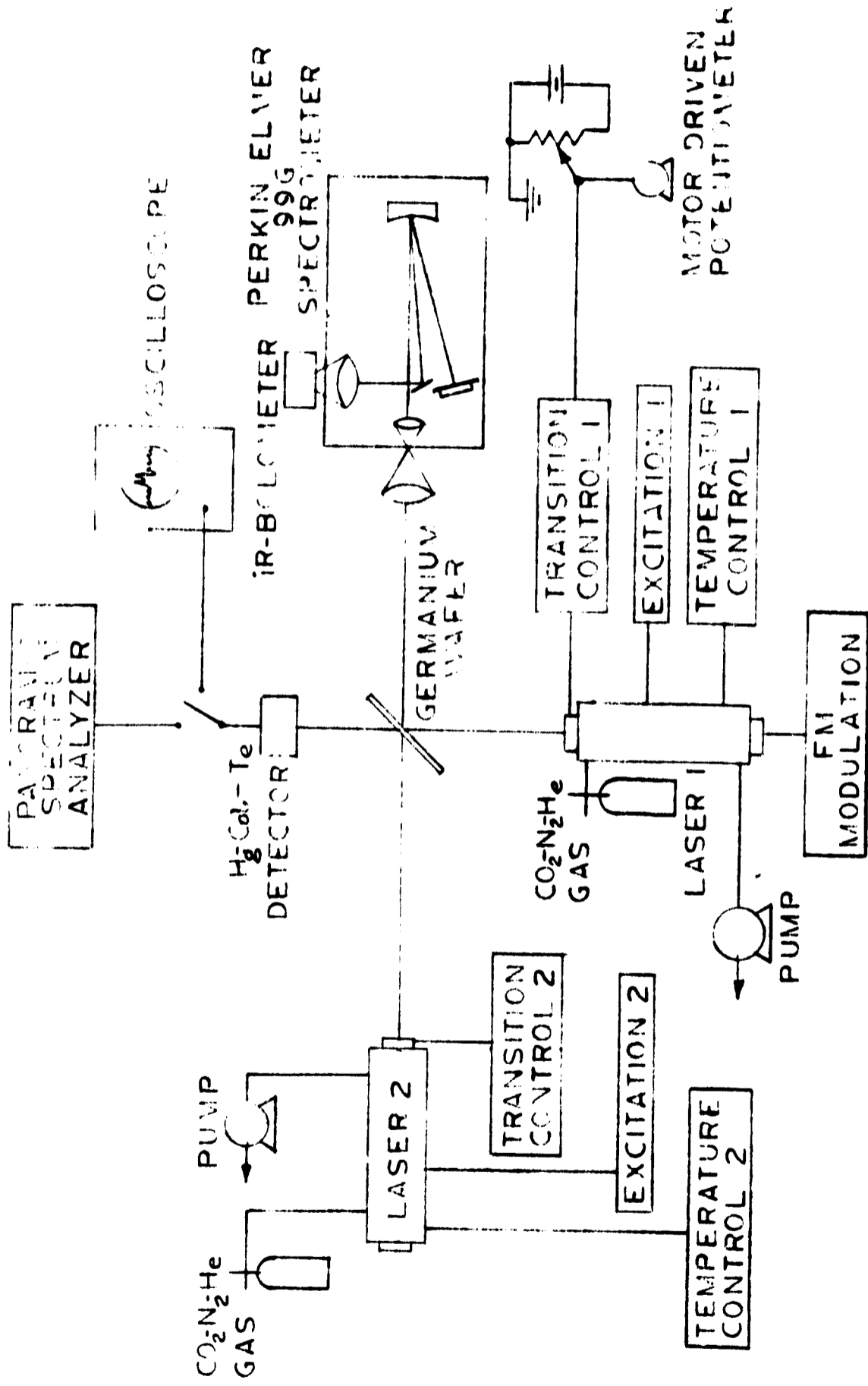


Figure 21. Optical Heterodyne Detection of the Beat Frequency of Two Stable CO<sub>2</sub> Lasers

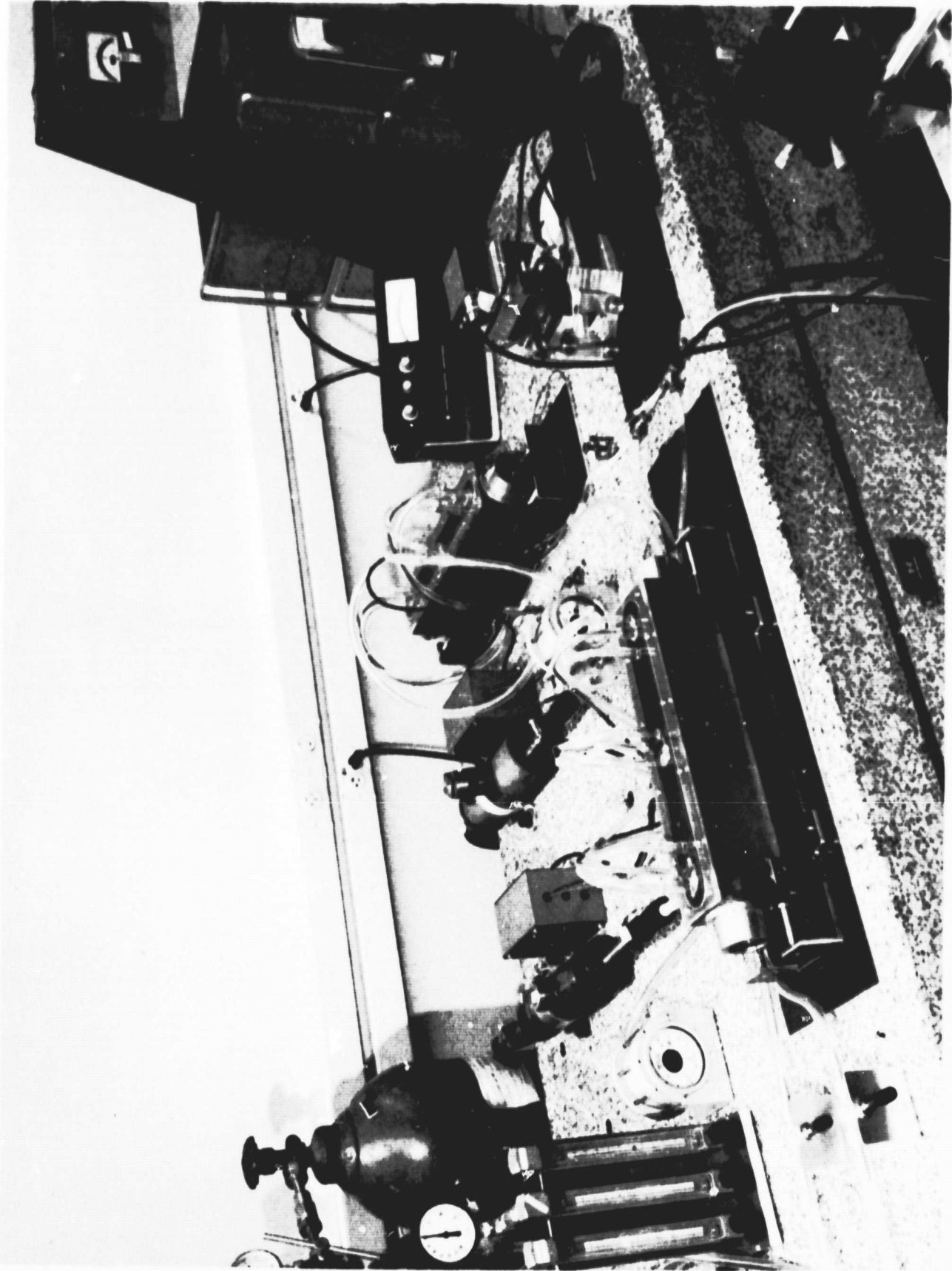
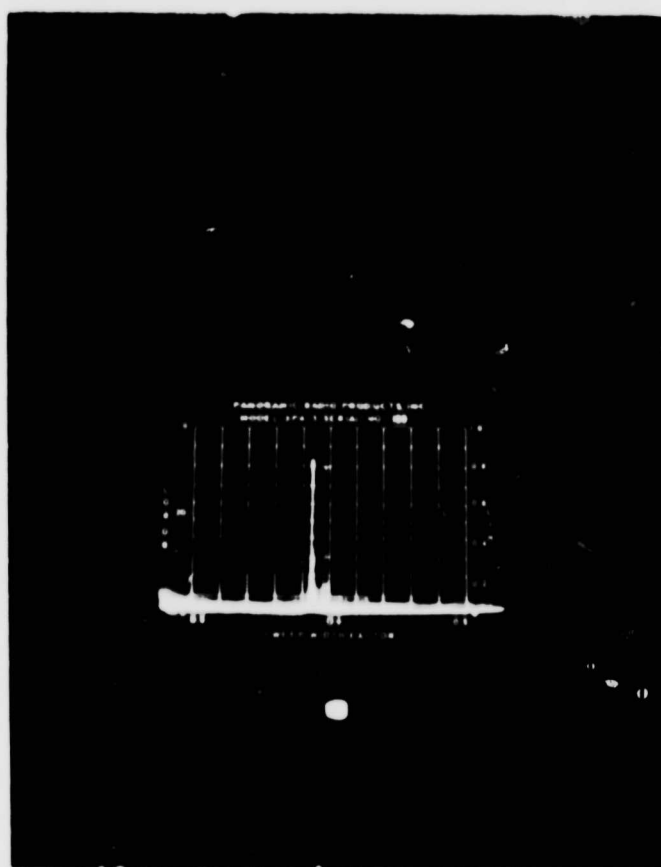


Figure 22. Optical Heterodyne Setup Mounted on Granite Slab

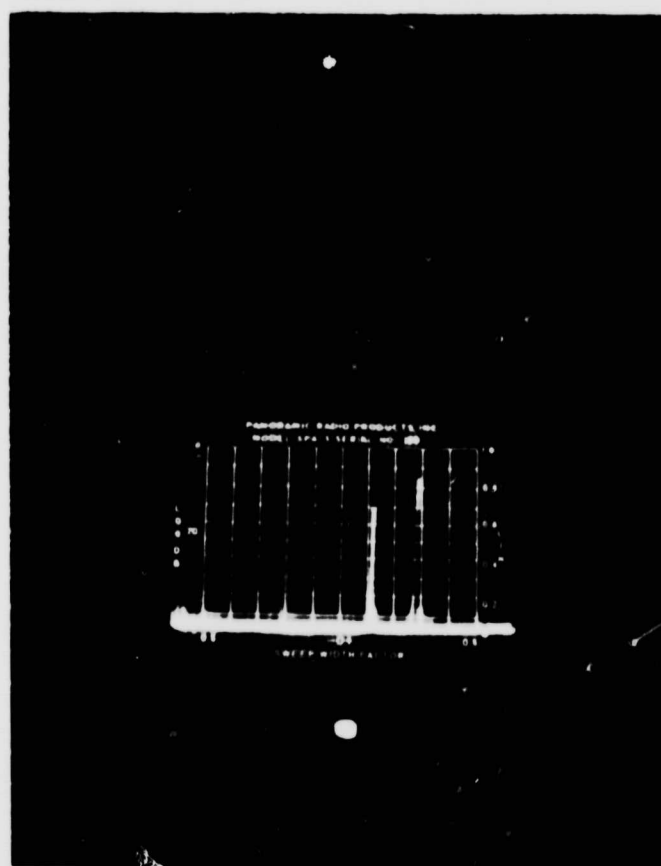
systems, was such that they would remain in oscillation at a desired transition, for an entire day. In general, we can say that the observed beat spectra did not show any difference with respect to short and long-term stability when the pair of lasers was beating on different transitions. We therefore concentrated on those transitions that have the largest output power, or on a pair where at least one laser does not need any bias voltage at all. Narrow frequency intervals where more than one frequency can oscillate simultaneously have been avoided. Over more than 95 percent of the cavity mode spacing ( $= 427$  MHz), both lasers emit a pure single frequency and no self-beat of either laser was observed on the spectrum analyzer. Both lasers could be set-off with respect to each other by frequencies ranging from 0 to 26 MHz on all transitions of interest P(16) to P(22). The limitation is given by the spectrum analyzer whose calibrated range stops at 26 MHz.

The results of the beat experiments can be summarized as follows: the relative short-term stability of the lasers without any AFC control and without water cooling is on the order of 2 to 3 kHz/sec over a time interval of 1/10 sec. This corresponds to a stability of  $S(t) = 10^{10}$  over this time interval. This represents the same short-term stability that has been obtained in the air-cooled version. Figure 23 shows a spectrum analyzer display with a resolution of 10 kHz/cm and 1/10 sec exposure time when the lasers are beating on the P(22) transition. The stability over one second is shown in Figure 24. The frequency fluctuations have increased to 25 kHz over the one second time interval. This is a factor 2 to 3 times larger than was expected. However the frequency spectrum of the fluctuation is on the order of 5 to 14 Hz and the AFC loop should be able to compensate for the fluctuations.

To improve the long-term stability we have connected both lasers (in parallel) to a Lear-Siegler water recirculating system. The long-term stability over minutes or hours is improved from  $10^7$  for the air-cooled laser to  $10^8$  for the water-cooled laser. However the short-term fluctuations (over one second) are increased from 30 kHz to 300 kHz. Long and short-term



(a)



(b)

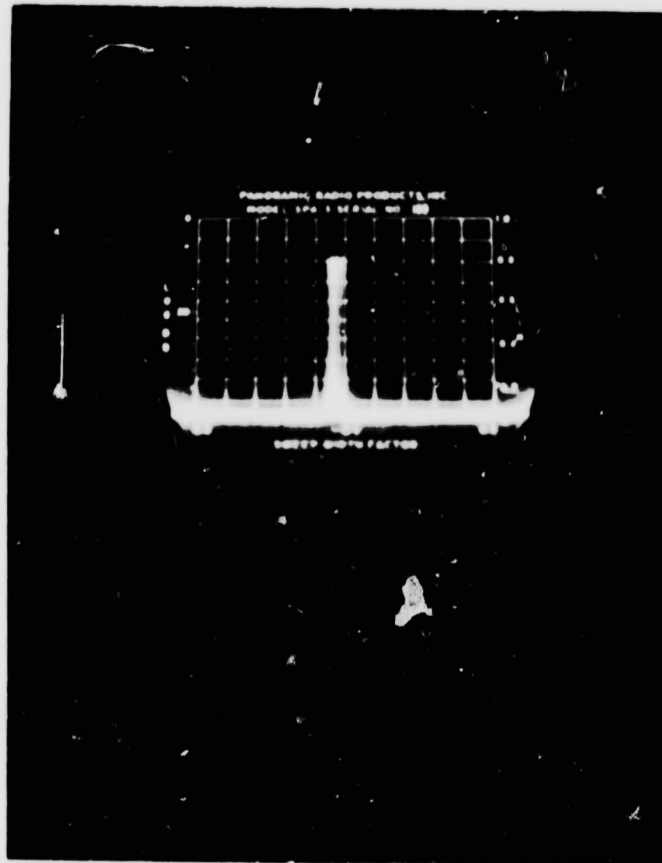
Figure 23. Both Lasers Beating on the P(22) - Transition  
Horizontal Dispersion 10 k Hz/cm. Exposure  
Time: 1/10 sec. Beat Frequency 4.2 MHz  
30 db Signal Attenuation, No Water Cooling



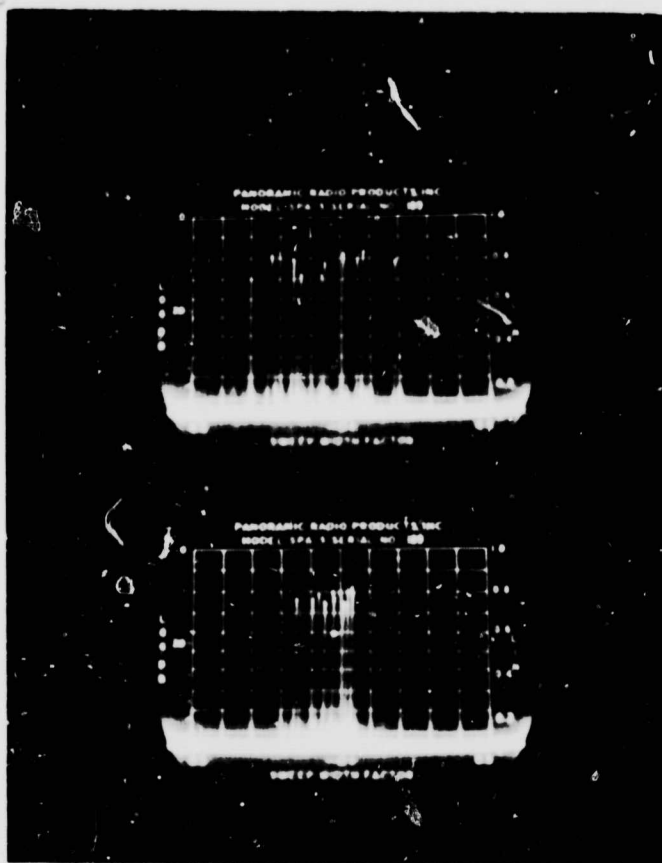
stability therefore is almost identical. Figure 25 shows the one second stability for both lasers beating on the P(20) transition; in Figure 25 (a) no water is circulating while in Figure 25 (b), the water circulator is turned on. The frequency fluctuations increase by a factor 5 to 10. The frequency fluctuations arise from pressure fluctuations generated by the pump of the circulator. These pressure fluctuations lead to small length-perturbations of the cavity. Without trying to correct these pressure fluctuations in the Lear-Siegler circulator we have used as coolers two Lauda temperature controllers with a listed accuracy of  $\pm 0.01^\circ\text{C}$ . These temperature controllers also generated sufficient pressure fluctuations to broaden the spectrum by almost an order of magnitude. Figure 26(a) and (b) show the frequency fluctuations with and without the temperature controllers in operation.

The problem of pressure fluctuations will be overcome by using pure "gravity" water flow through the lasers in order to decouple the cavity from pressure fluctuations of any pump. Some of the remaining fluctuations with water turned off were traced to gas flow fluctuations within the discharge tube. An improvement is possible by spatially separating the gas inlets and outlets from the electrodes, especially from the cathode.

Laser No. 1 oscillates over a narrow frequency interval on the transitions P(22) and P(30) simultaneously. Due to spatial competition one of the transitions is pushed into oscillation of a higher order off-axis mode  $\text{TEM}_{00q}$  and as a result we obtained a selfbeat at approximately 2.4 MHz. Figure 27(a) shows the narrow self-beat of laser No. 1 and Figure 27(b) in a lower resolution display the self-beat in the presence of the wider beat-signal of the P(22) transition which is also oscillating in laser No. 2.



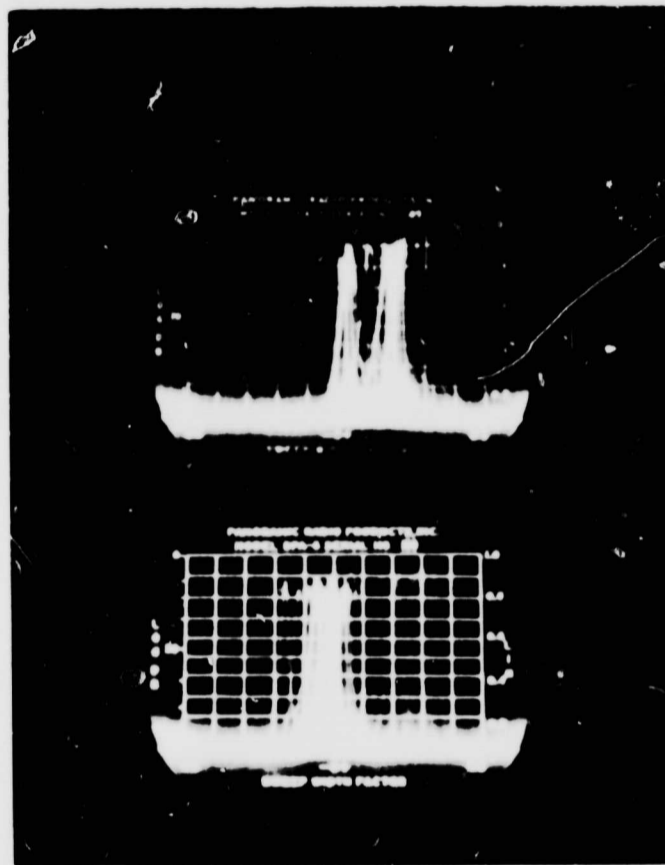
(a)



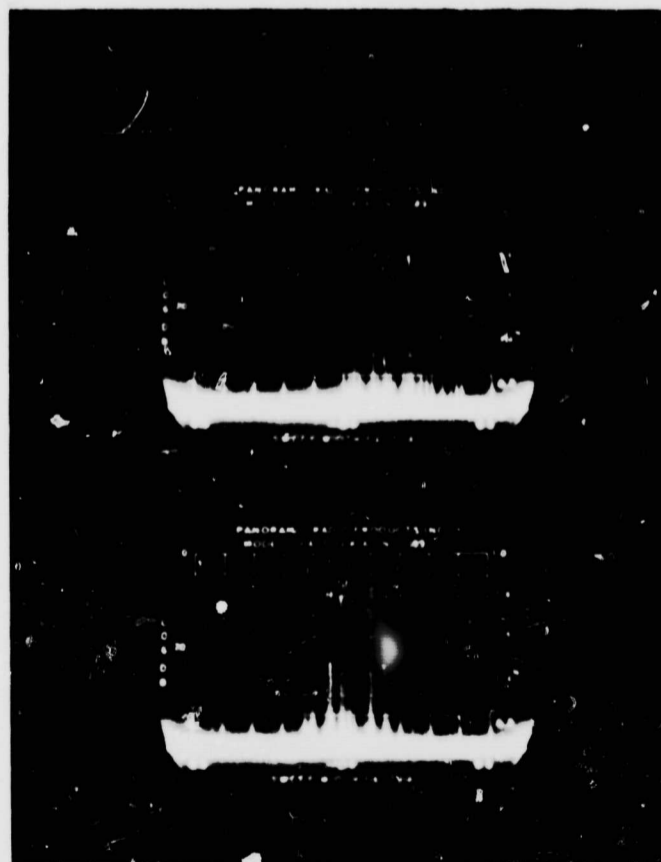
(b)

Figure 25. Both Lasers Beating on F(20) - Transition  
Horizontal Dispersion 50 k Hz/cm. Exposure:  
One Second, 30 db Attenuation  
(a) No Water Circulation  
(b) Both Lasers in Parallel, Cooled by Lear-  
Siegler Water Circulator





(a)



(b)

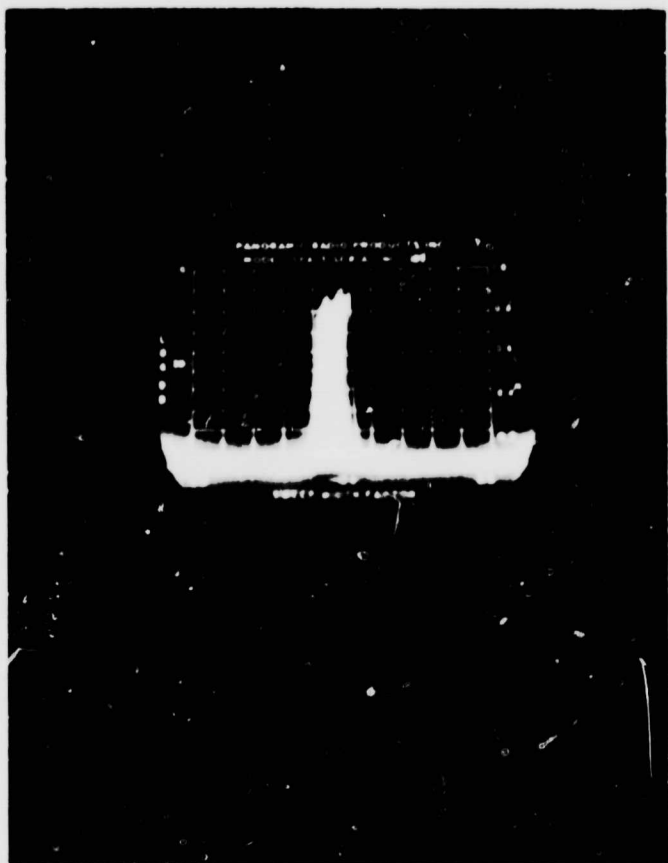
Figure 26. Both Lasers Beating on P(18) - Transition  
Horizontal Dispersion (a) 10 k Hz/cm  
(b) 100 k Hz/cm

Exposure Time: One Second

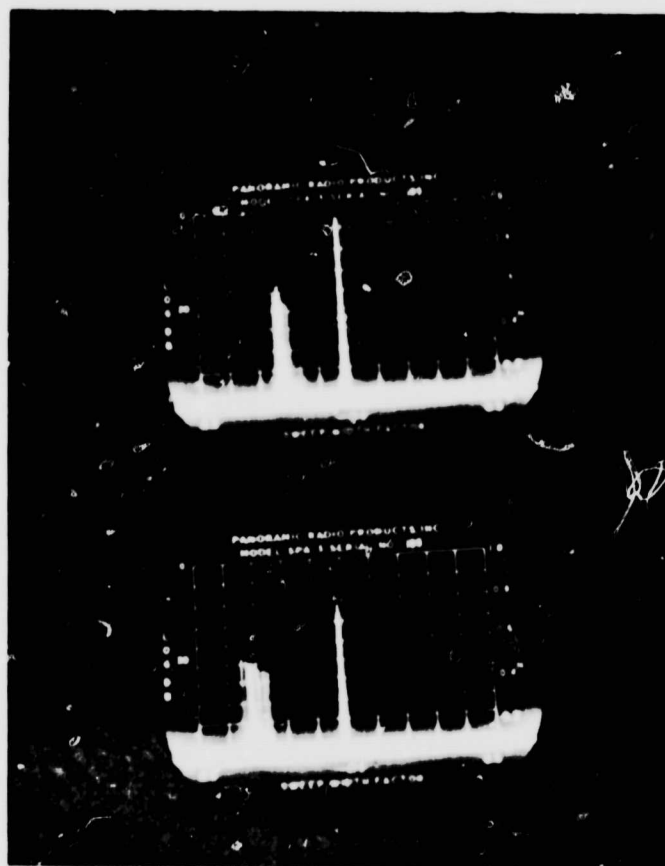
(a) No Water Circulation

(b) Each Laser Cooled by Lauda Temperature  
Controller

12044-PR4



(a)



(b)

Figure 27. (a) Self-beat of Laser No. 1 When Adjusted Piezoelectrically to Oscillate on Transition P(22) and P(30) Simultaneously.

Horizontal Dispersion 10 k Hz/cm  
Exposure Time: One Second

(b) Self-beat (in center) in the Presence of the True Beat Signal for Both Lasers Oscillating on P(22) Transition

Horizontal Dispersion 300 k Hz/cm  
Exposure Time: One Second  
Both Lasers Cooled with Lauda Temperature Controllers

REFERENCES

1. P.A. Miles, "Research Study of a CO<sub>2</sub> Laser Radar Transmitter," Raytheon Report AD 653 725.
2. F. Horrigan, "High Power Gas Laser Research," Raytheon Report AD 637 023.
3. D. R. Whitehouse, "High Power Gas Laser Research," Raytheon Report AD 653 031.
4. T.F. Deutsch, IEEE Journ. Quant. Electronics, QE-3, No. 4, April 1967.
5. C.K.N. Patel, Phys. Rev., Vol. 136, No. 5A, 30 November 1964.
6. Y.A. Howe, Appl. Phys. Letters, Vol. 7, No. 1, 1 July 1965.
7. T.J. Bridges, Appl. Phys. Letters, Vol. 9, No. 4, 15 August 1966.